AIMS Mathematics

https://www.aimspress.com/journal/Math

AIMS Mathematics, 11(8): 26026–26076.
DOI: 10.3934/math.20261043
Received: 09 June 2026
Revised: 18 July 2026
Accepted: 29 July 2026
Published: 20 August 2026

Research article

Reliability analysis for an independent Gompertz competing risks model employing improved adaptive progressive Type-II censored data

Hana N. Alqifari*

Department of Statistics and Operations Research, College of Science, Qassim University, Saudi Arabia

* **Correspondence:** Email: hn.alqifari@qu.edu.sa.

Abstract: In engineering life tests, units frequently fail from several competing causes, such as electrical breakdown competing with surface erosion in an insulation system, while cost and time constraints require censored designs that guarantee both a fixed number of observed failures and a bounded test duration. Statistical inference for competing risks' data under such adaptive censoring schemes remains challenging because the censoring mechanism and latent failure causes jointly complicate parameter estimation. The improved adaptive Type II progressive censoring scheme (IAT-II PCS) satisfies both design requirements simultaneously, yet, to the best of our knowledge, no peer-reviewed inferential framework has been developed for Gompertz competing risks data under this scheme, despite the flexibility of the Gompertz distribution in modeling exponentially increasing hazard rates, which differ from the power-law hazard of the Weibull distribution and cannot be captured by the constant hazard of the exponential model. This paper develops unified classical and Bayesian inference for this model. Exploiting the log-linear structure of the Gompertz likelihood, closed-form maximum likelihood estimators are derived for the cause-specific scale parameters, reducing the optimization to a one-dimensional profile search, and exact Gamma full conditional posteriors are obtained, enabling an efficient hybrid Gibbs–Metropolis–Hastings sampler. A Monte Carlo simulation study shows that Bayesian estimators under moderately informative priors generally outperform maximum likelihood in finite samples, with substantially improved mixing for the scale parameters. Application to an electrode voltage–endurance dataset demonstrates that the Gompertz model provides a superior joint likelihood fit relative to the Weibull alternative, confirming its practical value for censored reliability analysis.

Keywords: Gompertz distribution; competing risks; improved adaptive Type II progressive censoring; maximum likelihood estimation; hybrid MCMC; reliability analysis; simulation
Mathematics Subject Classification: 62N05, 62F15, 62F10

1. Introduction

In reliability engineering, industrial quality control, and biomedical research, it is rarely feasible to observe the complete failure history of all test units. Censoring mechanisms that allow early termination of life tests while preserving inferential validity are therefore essential. The progressive Type II censoring scheme (PCS-T2), formalized by [4] and accompanied by a practical simulation algorithm developed by [5], permits the random withdrawal of surviving units at pre-specified intermediate failure times through a censoring vector $\mathbf{R} = (R_1, \ldots, R_m)$, with $\sum_{i=1}^{m} R_i + m = n$. PCS-T2 encompasses conventional Type I and Type II censoring as special cases and reduces experimental costs while preserving statistical efficiency relative to complete-sample methods.

A recognized limitation of PCS-T2 is that the total experiment duration can be prohibitively long for highly reliable components. The progressive Type II hybrid censoring scheme (PHCS-T2) of [19] imposes a fixed termination time T, but at the cost of a random—potentially very small—effective sample size, which can severely compromise inferential precision. Ng et al. [22] proposed the adaptive progressive Type II censoring scheme (APCS-T2), which updates the censoring vector dynamically once a threshold time is exceeded, guaranteeing exactly m observed failures but without bounding the experiment's duration. Inference under APCS-T2 has since been developed for several lifetime models; for example, Sobhi and Soliman [26] derived estimators for the exponentiated Weibull distribution, and Ren and Gui [24] analyzed Weibull competing risks data under this scheme.

To simultaneously guarantee a pre-specified effective sample size and a finite termination time, Yan et al. [28] introduced the improved adaptive Type II progressive censoring scheme (IAT-II PCS). By incorporating a hard upper threshold T_2 alongside a lower threshold T_1, the IAT-II PCS ensures the experiment's termination no later than T_2 while subsuming PCS-T2, PHCS-T2, and APCS-T2 as special cases, making it a highly flexible member of the progressive Type II censoring family. Since its introduction, the IAT-II PCS has attracted rapidly growing research attention. Elshahhat and Nassar [14] developed inference for Weibull competing risks data under this scheme, while Dutta and Kayal [12] studied a competing risks model with exponential latent lifetimes. More recently, Alotaibi et al. [2] examined the Burr-X competing risks model, and Alotaibi et al. [3] studied the Nadarajah–Haghighi competing risks model, both under IAT-II PCS. Lone [34] developed maximum likelihood and Bayesian inference for the Burr Type III model under improved adaptive progressive censoring, and Wang [33] investigated heterogeneous competing risks under IAT-II PCS assuming Chen–Weibull latent lifetime distributions. Nevertheless, statistical inference for competing risks models under the improved adaptive progressive Type II censoring scheme remains relatively limited.

Competing risks data arise naturally in modern engineering systems, biomedical studies, and industrial reliability experiments where multiple failure modes act simultaneously. In electronic components, insulation breakdown due to thermal stress competes with mechanical fatigue; in oncological trials, cancer-specific mortality competes with cardiovascular death; in structural systems, corrosion competes with fatigue crack propagation [9, 20]. In each setting, the observed unit lifetime is the minimum of the latent failure times under each competing cause, and the operative cause is identified only at failure. Accurate cause-specific inference directly informs maintenance scheduling, warranty policy, and clinical treatment decisions. The canonical statistical framework is the latent failure time (LFT) model of [7], under which the independence of the latent failure times maintained throughout this paper simplifies the joint likelihood and enables cause-specific inference [9]. Parametric competing risks inference under progressive censoring has been studied for the Weibull distribution by Pareek et al. [23] and for the Lomax distribution by Cramer and Schmiedt [8]. Under adaptive schemes, Ren and Gui [24] analyzed Weibull competing risks, whereas Lv et al. [32] and Almuqrin et al. [1] studied Gompertz competing risks under general and adaptive progressive Type II censoring, respectively.

The Gompertz distribution, introduced by Gompertz [16] to model human mortality, is one of the most widely adopted lifetime distributions in actuarial science, demography, cancer research, and reliability engineering. Its prominence rests on several analytically attractive properties. First, its cumulative distribution function (CDF), survival, and quantile functions are all available in closed form, facilitating exact likelihood construction and efficient random variate generation. Second, its hazard rate function $h(x;\theta,\lambda) = \lambda e^{\theta x}$ is exponentially increasing for $\theta > 0$, a feature that distinguishes it from the Weibull distribution whose hazard rate follows a power law, and is particularly appropriate for modeling senescence, cumulative thermal damage, and accelerating fatigue; as $\theta \to 0$, the Gompertz reduces to the exponential distribution, providing a natural and testable nested hierarchy. From a practical perspective, the Gompertz model is expected to outperform the Weibull and exponential alternatives when the failure rate accelerates rapidly with age, as commonly occurs in wear-out and senescence processes. In contrast, the exponential model assumes a constant hazard, whereas the Weibull hazard evolves according to a power law. Such settings naturally favor the Gompertz model, whose hazard increases exponentially over time. This expectation is supported by the electrode voltage–endurance data analyzed in Section 7, where the Gompertz model achieves smaller Akaike information criterion (AIC) and Bayesian information criterion (BIC) values than the Weibull alternative. Third, the Gompertz distribution has been successfully applied to cancer survival datasets and electronic component failure data, demonstrating its practical versatility across reliability and biomedical contexts [18, 25]. Fourth, and most importantly for this paper, the Gompertz log-likelihood under competing risks has a distinctive analytical structure that leads directly to closed-form maximum likelihood estimators for the cause-specific scale parameters and to closed-form Gamma full conditional posteriors, properties that make both classical and Bayesian inference substantially more tractable than for other distributions studied under IAT-II PCS competing risks frameworks. Within this competing risks setting, Gompertz lifetimes have previously been examined under Type I progressive hybrid censoring by [27], under general progressive Type II censoring by [32], and under APCS-T2 by [1]. For single-population Gompertz data, Lone and Panahi [35] studied partially accelerated life testing under unified hybrid censoring, while Asadi et al. [36] considered adaptive progressive hybrid censored accelerated life tests. Further Type II progressive hybrid analyses of Gompertz lifetimes are given in [13, 21]. A preliminary conference poster by Dey et al. [10] outlined classical and Bayesian parameter estimation for independent Gompertz competing risks under IAT-II PCS and was presented at the International Workshop on Reliability Theory and Survival Analysis in December 2024. A substantially expanded preprint by the same authors [11] was posted on arXiv on 2 August 2026, while the present paper was awaiting publication. The expanded work emphasizes the existence and uniqueness of the maximum likelihood estimators, likelihood-ratio testing, multiple loss functions, and optimal censoring plans. The present study was developed independently and has a complementary reliability-oriented and computational focus: It derives explicit delta method confidence intervals for the reliability and hazard functions, quantitatively evaluates MCMC mixing efficiency, includes prior-sensitivity and small-sample analyses, and provides an engineering application with a systematic comparison against the Weibull competing risks model.

From a computational perspective, conditional on the shape parameter θ, the full conditional posteriors of the cause-specific scale parameters λ_1 and λ_2 are standard Gamma distributions, enabling direct Gibbs sampling without rejection, while only θ requires a Metropolis–Hastings (MH) step. This partially conjugate structure, which is not available in the Weibull, Nadarajah–Haghighi, and heterogeneous Chen–Weibull competing risks formulations studied under IAT-II PCS [3,14,33], yields improved mixing for the scale parameters, as documented quantitatively in the simulation study.

Despite the growing literature on competing risks models under IAT-II PCS, several reliability-oriented and computational aspects remained underdeveloped. In particular, the literature did not provide an integrated treatment combining explicit delta method inference for the reliability and hazard functions, quantitative assessment of MCMC mixing efficiency, prior-sensitivity and small-sample analyses, and a systematic Gompertz–Weibull goodness-of-fit comparison in an engineering application. The present paper addresses these limitations through the methodological, inferential, and applied contributions summarized below.

Contributions. The contributions of this paper span methodological, inferential, and applied dimensions. The main contributions of this paper are as follows.

1. Methodological: I formulate the independent Gompertz competing risks model under IAT-II PCS using the LFT framework and derive the corresponding three-case likelihood function, in which the failure cause indicators enable a separate estimation of the cause-specific scale parameters.

2. Classical inference: I derive closed-form maximum likelihood estimators for the cause-specific scale parameters as explicit functions of θ, reducing the full optimization to a one-dimensional profile search, and construct asymptotic confidence intervals (ACIs) for all parameters, $S(t)$, and $h(t)$ via the observed Fisher information matrix and the delta method, with all gradient expressions given in closed form.

3. Bayesian inference: I establish closed-form Gamma full conditional posteriors for λ_1 and λ_2 and develop a hybrid Gibbs–MH sampler in which only θ requires an MH step with an explicit Hastings correction; HPD credible intervals are computed via [6].

4. Simulation study: I conduct a Monte Carlo simulation study over a full factorial design of sample sizes, censoring schemes, and threshold settings, evaluating RMSE, MRAB, ACL, coverage probability, and ESS to document the finite-sample performance and computational advantages of the proposed methods.

5. Application: I apply the model to a real competing risks dataset and carry out a systematic goodness-of-fit comparison with the Weibull distribution across three IAT-II PCS censoring configurations.

Table 1 positions the present study among closely related competing risks and IAT-II PCS formulations. It provides a reliability-oriented unified classical and Bayesian treatment of an independent Gompertz competing risks model with a common shape parameter and cause-specific scale parameters under IAT-II PCS, distinguished by its delta method inference for the reliability and hazard functions, its quantitative assessment of MCMC mixing efficiency, and its comparative engineering application. The closed-form cause-specific scale estimators and the Gamma full conditional distributions are useful analytical features of this formulation, not features claimed to be unique across all such models. The preliminary poster and expanded preprint of Dey et al. [10, 11] are included in Table 1 for completeness.

Table 1. Positioning of the present study relative to related competing risks and IAT-II PCS formulations.

Study	Distribution	Scheme	Risk setting	Parameter structure	Classical / Bayesian computation
Yan et al. [28]	Burr-XII	IAT-II PCS	Single risk	Two shape parameters	Numerical MLE, bootstrap / MH within Gibbs
Dutta & Kayal [12]	Exponential	IAT-II PCS	Competing	Cause-specific rates	Fully closed-form / direct Gamma sampling
Elshahhat & Nassar [14]	Weibull	IAT-II PCS	Competing	Common shape, cause-specific scales	Closed-form scales + 1-D profile / Gibbs for scales, MH for shape
Alotaibi et al. [2]	Burr-X	IAT-II PCS	Competing	Cause-specific lifetime parameters	Numerical MLE / MCMC
Alotaibi et al. [3]	Nadarajah–Haghighi	IAT-II PCS	Competing	Cause-specific lifetime parameters	Numerical MLE / MH
Wang [33]	Chen–Weibull (heterogeneous)	IAT-II PCS	Competing	Distinct families, cause-specific parameters	Numerical MLE, bootstrap / MCMC
Lv et al. [32]	Gompertz	GPCS-T2	Competing	Cause-specific lifetime parameters	Numerical MLE, bootstrap / MCMC
Almuqrin et al. [1]	Gompertz	APCS-T2	Competing	Cause-specific lifetime parameters	NR and SEM / MH
Dey et al. [10, 11] (2024 poster; 2026 preprint)	Gompertz	IAT-II PCS	Competing	Common shape, cause-specific scales	Closed-form scales + fixed point / Gibbs for scales, MH for shape; LRT, optimality
Present study	**Gompertz**	**IAT-II PCS**	**Competing**	**Common shape, cause-specific scales**	**Closed-form scales + 1-D profile / Gibbs for scales, MH for shape; delta method ACIs for $S(t)$, $h(t)$; ESS/mixing analysis; Weibull goodness-of-fit study**

*Note: MLE = maximum likelihood estimator; MCMC = Markov chain Monte Carlo; MH = Metropolis–Hastings; NR = Newton–Raphson; SEM = stochastic expectation–maximization; GPCS-T2 = general progressive Type II censoring scheme; LRT = likelihood-ratio test.

The remainder of the paper is organized as follows. Section 2 describes the Gompertz distribution and the competing risks model. Section 3 presents the IAT-II PCS framework and derives the likelihood function. Sections 4 and 5 develop the classical and Bayesian estimation procedures, respectively. Section 6 reports the Monte Carlo simulation study. Section 7 presents the real data application. Section 7.6 provides a comparative analysis with the Weibull distribution. Section 8 concludes the paper.

2. Model description

2.1. The Gompertz distribution

Suppose that the lifetime of a test unit X follows the two-parameter Gompertz distribution $\mathrm{GZ}(\theta, \lambda)$, where $\theta > 0$ is the shape (acceleration) parameter and $\lambda > 0$ is the scale parameter. The probability density function (PDF), CDF, survival function (SF), and hazard rate function (HRF) are, respectively

$$f(x; \theta, \lambda) = \lambda\, e^{\theta x} \exp\Big\{\tfrac{\lambda}{\theta}(1 - e^{\theta x})\Big\}, \quad x > 0, \tag{2.1}$$

$$F(x; \theta, \lambda) = 1 - \exp\Big\{\tfrac{\lambda}{\theta}(1 - e^{\theta x})\Big\}, \quad x > 0, \tag{2.2}$$

$$S(x; \theta, \lambda) = \exp\Big\{\tfrac{\lambda}{\theta}(1 - e^{\theta x})\Big\}, \quad x \geq 0, \tag{2.3}$$

$$h(x; \theta, \lambda) = \lambda\, e^{\theta x}, \quad x \geq 0. \tag{2.4}$$

The hazard rate (2.4) is exponentially increasing for all $\theta > 0$, which distinguishes the Gompertz model from the Weibull distribution whose hazard rate follows a power law. As $\theta \to 0$, both (2.2) and (2.4) reduce to the exponential distribution with a rate λ, establishing the exponential as a nested special case. The quantile function, obtained by inverting $F(x) = u$, is

$$Q(u; \theta, \lambda) = \frac{1}{\theta} \log\Big\{1 - \frac{\theta}{\lambda} \log(1 - u)\Big\}, \quad u \in (0, 1), \tag{2.5}$$

which is used for random variate generation in the simulation study of Section 6.

2.2. Competing risks model

Let $X_1, \ldots, X_n$ be the lifetimes of n identical units placed on a life test. Without loss of generality, two competing failure causes are assumed, so the observed lifetime of the i-th unit is

$$X_i = \min\{X_{1i},\, X_{2i}\}, \quad i = 1, \ldots, n, \tag{2.6}$$

where X_{ji} is the latent failure time of unit i under cause j. The model assumptions are as follows:

(A1) Independence. For each i, X_{1i} and X_{2i} are stochastically independent.

(A2) Identical distribution. The pairs (X_{1i}, X_{2i}) are independently and identically distributed (i.i.d.) across $i = 1, \ldots, n$.

(A3) Cause identification. At each failure, an indicator $\xi_i \in \{1, 2\}$ records the operative cause.

(A4) Gompertz marginals. $X_{ji} \sim \mathrm{GZ}(\theta, \lambda_j)$, $j = 1, 2$, with a common shape $\theta > 0$ and distinct scales $\lambda_1, \lambda_2 > 0$.

Remark 1. *(Joint survival function) Under* (A1) *and* (A4)*, the joint SF of* $X = \min\{X_1, X_2\}$ *is*

$$\begin{aligned} S(x; \theta, \lambda_1, \lambda_2) &= S_1(x; \theta, \lambda_1) \times S_2(x; \theta, \lambda_2) \\ &= \exp\Big\{\tfrac{\lambda_1}{\theta}(1 - e^{\theta x})\Big\} \times \exp\Big\{\tfrac{\lambda_2}{\theta}(1 - e^{\theta x})\Big\} \\ &= \exp\Big\{\tfrac{\lambda_1 + \lambda_2}{\theta}(1 - e^{\theta x})\Big\}, \quad x \geq 0. \end{aligned} \tag{2.7}$$

Expression (2.7) *is a Gompertz SF with a shape θ and a scale $\lambda_1 + \lambda_2$. This is a consequence of the Gompertz reproductive property under the minimum operation when the shape parameter is shared. The corresponding HRF of X is*

$$h(x; \theta, \lambda_1, \lambda_2) = (\lambda_1 + \lambda_2)\, e^{\theta x}, \quad x \geq 0. \tag{2.8}$$

Remark 2. *Although the marginal distribution of X depends on λ_1 and λ_2 only through their sum, the individual parameters are identified by the* joint *distribution of (X, ξ). Specifically, the cause-specific likelihood factor for a failure from cause j at time x is $f_j(x; \theta, \lambda_j)\, S_{3-j}(x; \theta, \lambda_{3-j})$, which involves λ_j through $\log \lambda_j$ independently of the sum $\lambda_1 + \lambda_2$. Without the cause indicators ξ_i, the individual parameters λ_1 and λ_2 are not separately identifiable. With cause indicators, the likelihood factors by cause, enabling separate and simultaneous estimation. The exponential competing risks model is recovered as $\theta \to 0$, yielding the classical result $\pi_1 = \lambda_1/(\lambda_1 + \lambda_2)$ [23].*

Remark 3. *The independence assumption* (A1) *may fail when competing failure mechanisms are influenced by common environmental or manufacturing factors, as may occur in the electrode data considered in Section 7. By the non-identifiability result of [31], dependence among latent failure times cannot be tested from competing risks' data alone; consequently, violations of* (A1) *may affect inference on the latent failure structure even when the observable data are adequately fitted. Dependence can be accommodated through copula-based or Marshall–Olkin-type models [9], which we identify as future work.*

Remark 4. *The common-shape assumption* (A4) *is standard in the competing risks literature under progressive and adaptive censoring. Analogous common-shape formulations are used for the Weibull model [14, 23, 24]. Related competing risk formulations have also been adopted for the Burr-X and Nadarajah–Haghighi models [2, 3]. The assumption is often reasonable when competing failure mechanisms evolve under a common operating environment, while the cause-specific scale parameters capture differences between failure modes. Moreover, it yields a parsimonious model whose parameters remain stably estimable under heavy censoring. Nevertheless, it should be regarded as a modeling approximation rather than a physical law, and extending the model to allow cause-specific shape parameters is left for future work.*

Table 2 summarizes the main notation used throughout the paper.

Table 2. Summary of the main notation used throughout the paper.

Symbol	Description	Symbol	Description
θ	Common shape parameter	λ_1, λ_2	Cause-specific scale parameters
$S(t)$	Reliability function	$h(t)$	Hazard rate function
π_1	Relative risk	n	Total number of test units
m	Effective number of failures	R_i	Number of units removed at the ith failure
(T_1, T_2)	Lower and upper thresholds	T^*	Experiment termination time
D_1, D_2	Numbers of failures from the two causes	$W(\theta)$	Profile-likelihood quantity
ACI	Asymptotic confidence interval	HPD	Highest posterior density interval
ESS	Effective sample size		

3. IAT-II PCS scheme and likelihood function

3.1. Scheme description

Before the experiment begins, the experimenter specifies the total number of units n, the desired failure count $m < n$, a censoring scheme $\mathbf{R} = (R_1, \ldots, R_m)$ with $R_i \geq 0$ and $\sum_{i=1}^{m} R_i + m = n$, and two time thresholds $0 < T_1 < T_2 < \infty$. At the i-th failure time $X_{i:m:n}$, the cause ξ_i is recorded and R_i surviving units are randomly removed. Three cases arise according to the relationship between $X_{m:m:n}$ and the thresholds.

Case I. ($X_{m:m:n} < T_1$) All m failures occur before T_1. The experiment terminates at $X_{m:m:n}$ and the remaining $R_m = n - m - \sum_{i=1}^{m-1} R_i$ units are withdrawn. This is equivalent to conventional PCS-T2.

Case II. ($T_1 \leq X_{m:m:n} \leq T_2$) Let k_1 denote the number of failures before T_1. For $i > k_1$, the censoring numbers are set to zero ($R_i = 0$) and the experiment terminates at $X_{m:m:n}$. This is equivalent to APCS-T2.

Case III. ($X_{m:m:n} > T_2$) The experiment is stopped at T_2. Let k_2 denote the number of failures before T_2; withdrawals are set to zero after failure k_1, and $R^* = n - k_2 - \sum_{i=1}^{k_1} R_i$ units are removed simultaneously at T_2.

Figure 1 illustrates the three possible outcomes of the IAT-II PCS scheme. Case I: All m failures occur before the lower threshold T_1 and the test terminates at $X_{m:m:n}$ (equivalent to PCS-T2). Case II: The mth failure falls in $[T_1, T_2]$, withdrawals after T_1 are set to zero, and the test terminates at $X_{m:m:n}$ (equivalent to APCS-T2). Case III: The mth failure would exceed T_2, so the test stops at T_2 with all remaining units withdrawn. Table 3 summarizes the notation used in the likelihood. We write E_2 for the total observed failures, $E_2^{(j)}$ for those due to cause j, E_1 for failures before T_1, T^* for the termination time, and B for the units withdrawn at T^*.

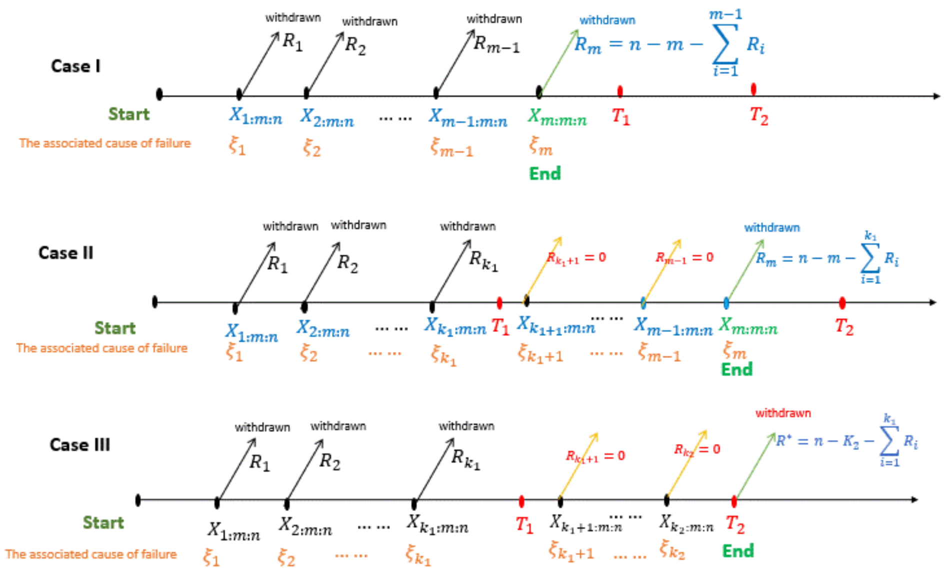

Figure 1. Schematic illustration of the improved adaptive Type II progressive censoring scheme.

3.2. Likelihood function

Under the latent failure time formulation with two independent competing causes, each unit contributes to the likelihood according to its observed status. A unit that fails at x_i from cause $\xi_i \in \{1,2\}$ contributes the cause-specific density of the failed latent cause together with the survival of the other, $f_{\xi_i}(x_i)\,S_{3-\xi_i}(x_i)$, since the competing cause is known only to have survived beyond x_i. Each of the R_i units progressively withdrawn at time x_i contributes the overall survival $S(x_i)^{R_i} = [S_1(x_i)S_2(x_i)]^{R_i}$, as such a unit is known only to have survived beyond x_i from both causes. Finally, the B units censored at the termination point T^* contribute $S(T^*)^B$. Multiplying these contributions over all observed failures and withdrawals, and substituting the corresponding values of (E_1, E_2, T^*, B) from Table 3, yields the unified likelihood in (3.1). The three cases differ only in their sample size at termination, the terminal time, and the number of units censored at the end of the experiment.

Table 3. IAT-II PCS likelihood notation.

Case	E_2	E_1	T^*	B
I	m	m	$X_{m:m:n}$	0
II	m	k_1	$X_{m:m:n}$	$n - m - \sum_{i=1}^{k_1} R_i$
III	k_2	k_1	T_2	$n - k_2 - \sum_{i=1}^{k_1} R_i$

Based on the observed IAT-II PCS competing risks data, the likelihood function is [14, 28]

$$L(\boldsymbol{\varphi} \mid \mathbf{x}) = C \prod_{i=1}^{E_2} [f_{\xi_i}(x_i)\,S_{3-\xi_i}(x_i)] \times \prod_{i=1}^{E_1} [S(x_i)]^{R_i} \times [S(T^*)]^B, \tag{3.1}$$

where $\boldsymbol{\varphi} = (\theta, \lambda_1, \lambda_2)^\top$; f_j and S_j denote the Gompertz PDF (2.1) and SF (2.3) with scale λ_j, respectively; $S(x) = S_1(x)S_2(x)$ is the joint SF (2.7); and C is a combinatorial constant free of the parameters. Let $\mathcal{I}_j = \{i : \xi_i = j\}$ for $j = 1, 2$.

Substituting (2.1), (2.3), and (2.7) into (3.1) and taking logarithms, the log-likelihood is

$$\ell(\boldsymbol{\varphi} \mid \mathbf{x}) = E_2^{(1)} \log \lambda_1 + E_2^{(2)} \log \lambda_2 + \theta \sum_{i=1}^{E_2} x_i - \frac{\lambda_1 + \lambda_2}{\theta}\, W(\theta), \tag{3.2}$$

where the sufficient statistic $W(\theta)$ is defined as

$$W(\theta) = \sum_{i=1}^{E_2} (e^{\theta x_i} - 1) + \sum_{i=1}^{E_1} R_i (e^{\theta x_i} - 1) + B(e^{\theta T^*} - 1). \tag{3.3}$$

A critical structural feature of (3.2) is that λ_1 and λ_2 appear through only three terms: $E_2^{(1)} \log \lambda_1$, $E_2^{(2)} \log \lambda_2$, and the joint term $-(\lambda_1 + \lambda_2)W(\theta)/\theta$. This decomposition directly enables the closed-form maximum likelihood estimators (MLEs) and Gamma full conditional posteriors derived in Sections 4 and 5.

4. Classical estimation

4.1. Maximum likelihood estimators

Setting the partial derivatives of $\ell(\boldsymbol{\varphi} \mid \mathbf{x})$ with respect to λ_1 and λ_2 to zero yields

$$\frac{\partial \ell}{\partial \lambda_1} = \frac{E_2^{(1)}}{\lambda_1} - \frac{W(\theta)}{\theta} = 0, \tag{4.1}$$

$$\frac{\partial \ell}{\partial \lambda_2} = \frac{E_2^{(2)}}{\lambda_2} - \frac{W(\theta)}{\theta} = 0. \tag{4.2}$$

Solving (4.1) and (4.2) directly gives closed-form MLEs for λ_1 and λ_2 as explicit functions of θ:

$$\hat{\lambda}_1(\theta) = \frac{E_2^{(1)}\,\theta}{W(\theta)}, \qquad \hat{\lambda}_2(\theta) = \frac{E_2^{(2)}\,\theta}{W(\theta)}. \tag{4.3}$$

Note that $\hat{\lambda}_1 + \hat{\lambda}_2 = E_2\,\theta/W(\theta)$, which is the MLE of the aggregated scale in the marginal Gompertz distribution of X. The profile log-likelihood in θ alone is obtained by substituting the closed-form estimators (4.3) back into the log-likelihood (3.2). The first two terms become $E_2^{(1)} \log \hat{\lambda}_1(\theta)$ and $E_2^{(2)} \log \hat{\lambda}_2(\theta)$, while the linear term $\theta \sum_{i=1}^{E_2} x_i$ remains unchanged. The only non-trivial simplification arises from the joint term involving $W(\theta)$. Using $\hat{\lambda}_1(\theta) + \hat{\lambda}_2(\theta) = E_2\,\theta/W(\theta)$, we have

$$-\frac{\hat{\lambda}_1(\theta) + \hat{\lambda}_2(\theta)}{\theta}\,W(\theta) = -\frac{1}{\theta} \cdot \frac{E_2\,\theta}{W(\theta)} \cdot W(\theta) = -E_2,$$

where the factors θ and $W(\theta)$ cancel. Collecting the three surviving contributions gives the profile log-likelihood

$$\ell_p(\theta) = E_2^{(1)} \log\left(\frac{E_2^{(1)}\theta}{W(\theta)}\right) + E_2^{(2)} \log\left(\frac{E_2^{(2)}\theta}{W(\theta)}\right) + \theta \sum_{i=1}^{E_2} x_i - E_2. \tag{4.4}$$

The MLE $\hat{\theta}$ is the maximizer of (4.4), obtained via the Newton–Raphson method using the `maxLik` package in `R` [17]. The full MLEs are then $\hat{\lambda}_1 = \hat{\lambda}_1(\hat{\theta})$ and $\hat{\lambda}_2 = \hat{\lambda}_2(\hat{\theta})$. By the invariance property of the MLE, the estimated reliability and HRF are

$$\hat{S}(t) = \exp\left\{\frac{\hat{\lambda}_1 + \hat{\lambda}_2}{\hat{\theta}}(1 - e^{\hat{\theta}t})\right\}, \tag{4.5}$$

$$\hat{h}(t) = (\hat{\lambda}_1 + \hat{\lambda}_2)e^{\hat{\theta}t}. \tag{4.6}$$

4.2. Relative risk

The relative risk for Cause 1 is $\pi_1 = P(X_1 < X_2)$, which, under the latent failure time formulation and the independence assumption, can be written as

$$\pi_1 = \int_0^\infty f_1(x)\,S_2(x)\,dx.$$

Substituting the Gompertz density (2.1) for f_1 and the corresponding SF (2.3) for S_2, and applying the change in the variable $u = e^{\theta x}$, for which $du = \theta e^{\theta x}\,dx$ so that $e^{\theta x}\,dx = du/\theta$, with the limits $x = 0 \mapsto u = 1$ and $x \to \infty \mapsto u \to \infty$:

$$\begin{aligned}
\pi_1 &= \int_0^\infty f_1(x;\theta,\lambda_1)\,S_2(x;\theta,\lambda_2)\,dx \\
&= \int_0^\infty \lambda_1 e^{\theta x}\exp\left\{\tfrac{\lambda_1+\lambda_2}{\theta}(1-e^{\theta x})\right\}dx \\
&= \frac{\lambda_1}{\theta}\,e^{(\lambda_1+\lambda_2)/\theta}\int_1^\infty e^{-[(\lambda_1+\lambda_2)/\theta]u}\,du \\
&= \frac{\lambda_1}{\theta}\,e^{(\lambda_1+\lambda_2)/\theta}\cdot\frac{\theta}{\lambda_1+\lambda_2}\,e^{-(\lambda_1+\lambda_2)/\theta} \\
&= \frac{\lambda_1}{\lambda_1+\lambda_2}.
\end{aligned} \tag{4.7}$$

The penultimate line uses $\int_1^\infty e^{-au}\,du = e^{-a}/a$ with $a = (\lambda_1+\lambda_2)/\theta > 0$, after which the exponential factors $e^{(\lambda_1+\lambda_2)/\theta}$ and $e^{-(\lambda_1+\lambda_2)/\theta}$ cancel, leaving a result that depends only on the ratio of the cause-specific scale parameters and is free of the common shape parameter θ.

The closed form $\pi_1 = \lambda_1/(\lambda_1+\lambda_2)$ holds for *all* $\theta > 0$. The relative risk depends only on the ratio of scale parameters and is independent of the shape parameter. The MLE is $\hat{\pi}_1 = \hat{\lambda}_1/(\hat{\lambda}_1+\hat{\lambda}_2) = E_2^{(1)}/E_2$, which equals the sample proportion of Cause 1 failures, consistent with maximum likelihood theory. The relative risk for Cause 2 is $\pi_2 = 1 - \pi_1$.

4.3. Asymptotic confidence intervals

Under standard regularity conditions, $\hat{\boldsymbol{\varphi}} \xrightarrow{d} N_3(\boldsymbol{\varphi}, \mathbf{I}^{-1}(\boldsymbol{\varphi}))$. The observed information matrix $\hat{\mathbf{I}}(\hat{\boldsymbol{\varphi}})$ has elements $-\partial^2\ell/\partial\varphi_i\partial\varphi_j$ evaluated at $\hat{\boldsymbol{\varphi}}$. From (3.2), we have

$$\ell_{11} = -\frac{E_2^{(1)}}{\lambda_1^2}, \quad \ell_{22} = -\frac{E_2^{(2)}}{\lambda_2^2}, \quad \ell_{12} = 0, \tag{4.8}$$

$$\ell_{13} = \ell_{23} = \frac{W(\theta)}{\theta^2} - \frac{W'(\theta)}{\theta}, \tag{4.9}$$

$$\ell_{33} = -\frac{\lambda_1+\lambda_2}{\theta}\,W''(\theta) + \frac{2(\lambda_1+\lambda_2)}{\theta^2}\,W'(\theta) - \frac{2(\lambda_1+\lambda_2)}{\theta^3}\,W(\theta), \tag{4.10}$$

where

$$W'(\theta) = \sum_{i=1}^{E_2} x_i e^{\theta x_i} + \sum_{i=1}^{E_1} R_i x_i e^{\theta x_i} + B\,T^* e^{\theta T^*}, \tag{4.11}$$

$$W''(\theta) = \sum_{i=1}^{E_2} x_i^2 e^{\theta x_i} + \sum_{i=1}^{E_1} R_i x_i^2 e^{\theta x_i} + B\,(T^*)^2 e^{\theta T^*}. \tag{4.12}$$

Note that $\ell_{12} = 0$ and $\ell_{13} = \ell_{23}$ because λ_1 and λ_2 enter (3.2) symmetrically through $(\lambda_1+\lambda_2)W(\theta)/\theta$. The approximate covariance matrix is $\hat{\mathbf{I}}^{-1}(\hat{\boldsymbol{\varphi}}) = -[\ell_{ij}]^{-1}|_{\boldsymbol{\varphi}=\hat{\boldsymbol{\varphi}}} = [\hat{\sigma}_{ij}]$. The two-sided $100(1-\gamma)\%$ ACI for φ_i is $\hat{\varphi}_i \pm z_{\gamma/2}\sqrt{\hat{\sigma}_{ii}}$, where $z_{\gamma/2}$ is the upper $(\gamma/2)$-quantile of the standard normal distribution. All entries of the observed information matrix are available in closed form and are evaluated analytically at $\hat{\varphi}$, which avoids numerical differentiation and the associated round-off error.

4.4. *Delta method ACIs for $S(t)$ and $h(t)$*

Define the gradient vectors $\nabla S = (\partial S/\partial\lambda_1,\ \partial S/\partial\lambda_2,\ \partial S/\partial\theta)^\top$ and $\nabla h = (\partial h/\partial\lambda_1,\ \partial h/\partial\lambda_2,\ \partial h/\partial\theta)^\top$. Differentiating (2.7) and (2.8), we have

$$\frac{\partial S}{\partial\lambda_1} = \frac{\partial S}{\partial\lambda_2} = \frac{1-e^{\theta t}}{\theta}\, S(t), \tag{4.13}$$

$$\frac{\partial S}{\partial\theta} = (\lambda_1+\lambda_2)\left[-\frac{t\,e^{\theta t}}{\theta} - \frac{1-e^{\theta t}}{\theta^2}\right] S(t), \tag{4.14}$$

$$\frac{\partial h}{\partial\lambda_1} = \frac{\partial h}{\partial\lambda_2} = e^{\theta t}, \tag{4.15}$$

$$\frac{\partial h}{\partial\theta} = (\lambda_1+\lambda_2)\, t\, e^{\theta t}. \tag{4.16}$$

Note that $\partial S/\partial\lambda_1 = \partial S/\partial\lambda_2$ and $\partial h/\partial\lambda_1 = \partial h/\partial\lambda_2$ because both functions depend on λ_1 and λ_2 only through the sum $\lambda_1+\lambda_2$ in (2.7) and (2.8). The approximate variances are

$$\hat{\sigma}_S^2 = \nabla\hat{S}^\top\, \hat{\mathbf{I}}^{-1}(\hat{\boldsymbol{\varphi}})\, \nabla\hat{S}, \qquad \hat{\sigma}_h^2 = \nabla\hat{h}^\top\, \hat{\mathbf{I}}^{-1}(\hat{\boldsymbol{\varphi}})\, \nabla\hat{h},$$

both evaluated at $\hat{\boldsymbol{\varphi}}$. The two-sided $100(1-\gamma)\%$ ACIs are $\hat{S}(t) \pm z_{\gamma/2}\hat{\sigma}_S$ and $\hat{h}(t) \pm z_{\gamma/2}\hat{\sigma}_h$.

5. Bayesian estimation

5.1. *Prior distributions and posterior*

We adopt the symmetric squared error loss (SEL) function $\ell(\eta,\tilde{\eta}) = (\eta-\tilde{\eta})^2$, under which the Bayes estimator is the posterior mean. Independent Gamma priors are assigned: $\lambda_j \sim \text{Gamma}(a_j, b_j)$ for $j = 1,2$, and $\theta \sim \text{Gamma}(a_3, b_3)$, giving the joint prior

$$g(\lambda_1,\lambda_2,\theta) \propto \lambda_1^{a_1-1}\lambda_2^{a_2-1}\theta^{a_3-1}\exp\{-(b_1\lambda_1 + b_2\lambda_2 + b_3\theta)\}. \tag{5.1}$$

The Gamma family is adopted for both the scale and the shape parameters because it is supported on the positive real line, its two hyperparameters flexibly encode weak or moderate prior information, and it is conditionally conjugate for the cause-specific scale parameters, yielding the closed-form Gamma full conditionals that underlie the efficient hybrid Gibbs step. Setting $a_i = b_i = 0$ for all i yields improper non-informative priors. The joint posterior is

$$\pi(\boldsymbol{\varphi} \mid \mathbf{x}) \propto L(\boldsymbol{\varphi} \mid \mathbf{x}) \cdot g(\lambda_1,\lambda_2,\theta). \tag{5.2}$$

The limiting choice $a_i = b_i = 0$ is introduced only as a non-informative reference and is not used in the simulation study or the real data application. The prior specifications adopted in this paper (Priors I and II) are proper Gamma distributions; consequently, the posterior distributions used throughout the paper are proper. Under the limiting improper specification, posterior propriety requires additional regularity conditions, including a proper prior on the common shape parameter θ, a condition satisfied by both Priors I and II.

5.2. Closed-form full conditional posteriors

Collecting all factors of the joint posterior (5.2) that involve λ_1:

$$\pi(\lambda_1 \mid \lambda_2, \theta, \mathbf{x}) \propto \lambda_1^{a_1+E_2^{(1)}-1} \exp\left\{-\lambda_1\left[b_1 + \frac{W(\theta)}{\theta}\right]\right\}. \tag{5.3}$$

Expression (5.3) is a Gamma kernel:

$$\lambda_1 \mid \lambda_2, \theta, \mathbf{x} \;\sim\; \Gamma\left(a_1 + E_2^{(1)},\; b_1 + \frac{W(\theta)}{\theta}\right). \tag{5.4}$$

By the same argument, we have

$$\lambda_2 \mid \lambda_1, \theta, \mathbf{x} \;\sim\; \Gamma\left(a_2 + E_2^{(2)},\; b_2 + \frac{W(\theta)}{\theta}\right). \tag{5.5}$$

The existence of closed-form Gamma full conditionals for λ_1 and λ_2 is a direct consequence of the log-linear structure of (3.2) in λ_1 and λ_2. This contrasts with the Weibull and Nadarajah–Haghighi competing risks models under IAT-II PCS [3, 14], where the scale parameters enter the likelihood through nonlinear power terms, making their full conditionals non-standard and requiring MH updates for all parameters. The Gompertz model therefore admits a more efficient hybrid Gibbs–MH sampler with exact draws for λ_1 and λ_2.

The full conditional for θ is non-standard.

$$\pi(\theta \mid \lambda_1, \lambda_2, \mathbf{x}) \propto \theta^{a_3-1} e^{-b_3\theta} \exp\left\{\theta \sum_{i=1}^{E_2} x_i - \frac{\lambda_1 + \lambda_2}{\theta}\, W(\theta)\right\}, \tag{5.6}$$

because θ enters (5.6) nonlinearly through $e^{\theta x_i}$ inside $W(\theta)$ and through $1/\theta$. Accordingly, θ is sampled via a log-scale random walk MH step.

5.3. Hybrid Gibbs–Metropolis–Hastings algorithm

Let $\boldsymbol{\varphi}^{(g-1)} = (\theta^{(g-1)}, \lambda_1^{(g-1)}, \lambda_2^{(g-1)})^\top$ denote the current state at iteration g. One complete iteration of the hybrid sampler proceeds as follows.

Step 1 (MH update for θ). Propose $\log\theta^* = \log\theta^{(g-1)} + \varepsilon_\theta$ with $\varepsilon_\theta \sim N(0, s_\theta^2)$. Compute the log-acceptance ratio with the Hastings correction for the log-scale proposal:

$$\log\alpha_\theta = \log\pi(\theta^* \mid \lambda_1^{(g-1)}, \lambda_2^{(g-1)}, \mathbf{x}) - \log\pi(\theta^{(g-1)} \mid \lambda_1^{(g-1)}, \lambda_2^{(g-1)}, \mathbf{x}) + \log\frac{\theta^*}{\theta^{(g-1)}}. \tag{5.7}$$

Generate $U_\theta \sim U(0,1)$. If $\log U_\theta < \log\alpha_\theta$ set $\theta^{(g)} = \theta^*$; otherwise, $\theta^{(g)} = \theta^{(g-1)}$.

Step 2 (Gibbs update for λ_1). Sample directly from the following closed-form full conditional (5.4):

$$\lambda_1^{(g)} \sim \text{Gamma}\left(a_1 + E_2^{(1)},\; b_1 + \frac{W(\theta^{(g)})}{\theta^{(g)}}\right). \tag{5.8}$$

Step 3 (Gibbs update for λ_2). Sample directly from (5.5).

$$\lambda_2^{(g)} \sim \text{Gamma}\left(a_2 + E_2^{(2)},\ b_2 + \frac{W(\theta^{(g)})}{\theta^{(g)}}\right). \tag{5.9}$$

Step 4 (Derived quantities). Compute posterior draws of the reliability function (RF) and HRF at mission time t:

$$S^{(g)}(t) = \exp\left\{\frac{\lambda_1^{(g)} + \lambda_2^{(g)}}{\theta^{(g)}}(1 - e^{\theta^{(g)}t})\right\}, \tag{5.10}$$

$$h^{(g)}(t) = (\lambda_1^{(g)} + \lambda_2^{(g)})e^{\theta^{(g)}t}. \tag{5.11}$$

Step 5. Set $g = g + 1$ and repeat Steps 1–4 for M iterations.

After generating M posterior samples, the first M_0 iterations are discarded as burn-in. The remaining $M - M_0$ samples are used to compute the Bayes estimates (posterior means), posterior standard deviations, and highest posterior density (HPD) credible intervals via the method of [6]. The step size s_θ controls the mixing of the θ chain and is selected by a pilot proposal-scale study (Section 6.6) that trades off the acceptance rate against the effective sample size, with the recommended range near an acceptance rate of ≈ 0.44, the optimum for a scalar random walk target [15]. The effective sample size (ESS) for each parameter is computed as $\text{ESS} = (M - M_0)/(1 + 2\sum_{k=1}^{\infty} \rho_k)$, where ρ_k is the lag-k autocorrelation of the posterior chain.

The hybrid structure provides three computational advantages over a fully MH-based sampler.

1. The Gibbs steps for λ_1 and λ_2 are exact (no rejection), yielding an ESS close to $(M - M_0)$ for these parameters after accounting for their dependence on θ.

2. The Markov chain mixes faster because the joint conditional distribution of (λ_1, λ_2) given θ is perfectly sampled at each iteration.

3. Only a single tuning parameter s_θ is required, simplifying practical implementation compared with fully MH-based algorithms that require separate step sizes for all parameters.

These advantages are documented quantitatively in Section 6 through the ESS values, trace plots, and autocorrelation functions.

6. Monte Carlo simulation study

6.1. Simulation design

A comprehensive Monte Carlo simulation study with $G = 1{,}000$ independent replications is conducted to evaluate the finite-sample performance of the proposed classical and Bayesian inferential procedures. The true parameter values are fixed as

$$\theta_0 = 1.5, \quad \lambda_{10} = 0.5, \quad \lambda_{20} = 1.0,$$

yielding the true reliability function and hazard rate at the mission time $t_0 = 0.5$ thousand hours:

$$S_0(t_0) = \exp\left\{\tfrac{1.5}{1.5}(1 - e^{0.75})\right\} \approx 0.3273, \qquad h_0(t_0) = 1.5\, e^{0.75} \approx 3.1755, \qquad \pi_{10} = \frac{0.5}{1.5} = 0.3333.$$

The following combinations of a total sample size n and an effective failure count m are considered:

$$(n, m) \in \{(40, 20),\ (40, 30),\ (80, 40),\ (80, 60)\}.$$

Four censoring schemes are examined for each (n, m) pair:

- **Scheme U** (Uniform): The removals are distributed as evenly as possible across the m failure times. When $(n - m)/m$ is an integer, we set $R_i = (n - m)/m$ for all i. Otherwise, writing $n - m = qm + s$ with $q = \lfloor (n - m)/m \rfloor$ and $s = (n - m) \bmod m$, set

$$R_i = \begin{cases} q + 1, & i = 1, \ldots, s, \\ q, & i = s + 1, \ldots, m, \end{cases} \qquad \text{so that } \sum_{i=1}^{m} R_i = n - m.$$

- **Scheme L** (Left-heavy): $R_1 = n - m$, $R_i = 0$ for $i > 1$.
- **Scheme M** (Middle): $R_{\lceil m/2 \rceil} = n - m$, $R_i = 0$ otherwise.
- **Scheme R** (Right-heavy): $R_m = n - m$, $R_i = 0$ for $i < m$.

Two threshold settings are considered as follows: $(T_1, T_2) = (0.4, 0.8)$ and $(T_1, T_2) = (0.8, 1.5)$. The full factorial design yields $2 \times 4 \times 4 = 32$ scenarios. The two threshold pairs were chosen to represent different operating regimes of the IAT-II PCS. The setting $(0.4, 0.8)$ corresponds to a relatively restrictive design in which the adaptive update and the time cap are more likely to affect the course of the experiment, whereas $(0.8, 1.5)$ represents a less restrictive design in which termination is more often driven by the target number of failures. Considering both settings allows the simulation study to assess the finite-sample behavior of the proposed estimators under different censoring patterns and across the three cases of the IAT-II PCS.

For each scenario, $G = 1{,}000$ independent IAT-II PCS samples are generated from the Gompertz competing risks model using the quantile function (2.5). For Bayesian estimation, the hybrid Gibbs–MH sampler is run with $M = 12{,}000$ iterations and a burn-in of $M_0 = 2{,}000$, yielding 10,000 posterior draws per replication. Two prior settings are considered as follows:

- **Prior I** (weakly informative): $a_j = b_j = 0.001$ for $j = 1, 2, 3$.
- **Prior II** (moderately informative): $a_1 = 10$, $b_1 = 20$, $a_2 = 20$, $b_2 = 20$, $a_3 = 30$, and $b_3 = 20$, chosen so that the prior means equal the true values, and the prior coefficients of variation equal 1.

Because the mean of Prior II is placed exactly at the data-generating parameter values, the results obtained under it should be read as a best-case benchmark, attainable only when accurate prior information is available. As such information is rarely available in practice, the robustness of the Bayesian procedure to prior misspecification is examined separately in Section 6.7.

6.2. Performance measures

For any estimator $\hat{\psi}$ of a scalar quantity ψ, the root mean squared error (RMSE) and mean relative absolute bias (MRAB) are

$$\mathrm{RMSE}(\hat{\psi}) = \left[\frac{1}{G}\sum_{g=1}^{G}(\hat{\psi}^{(g)} - \psi)^2\right]^{1/2}, \qquad \mathrm{MRAB}(\hat{\psi}) = \frac{1}{G}\sum_{g=1}^{G}\left|\frac{\hat{\psi}^{(g)} - \psi}{\psi}\right|. \tag{6.1}$$

Point estimation entries are reported as $\overline{\hat{\psi}}$ (RMSE, MRAB). For interval estimation, the average confidence length (ACL) and coverage probability (CP) are reported as ACL (CP). For the Bayesian sampler, the ESS and MH acceptance rate for θ are also reported.

6.3. MCMC convergence diagnostics

Figure 2 presents trace plots (top row) and autocorrelation function (ACF) plots (bottom row) for the posterior draws of λ_1, λ_2, θ, $S(t_0)$, and $h(t_0)$ under the representative setting $(n, m) = (40, 20)$, Scheme U, and $(T_1, T_2) = (0.4, 0.8)$.

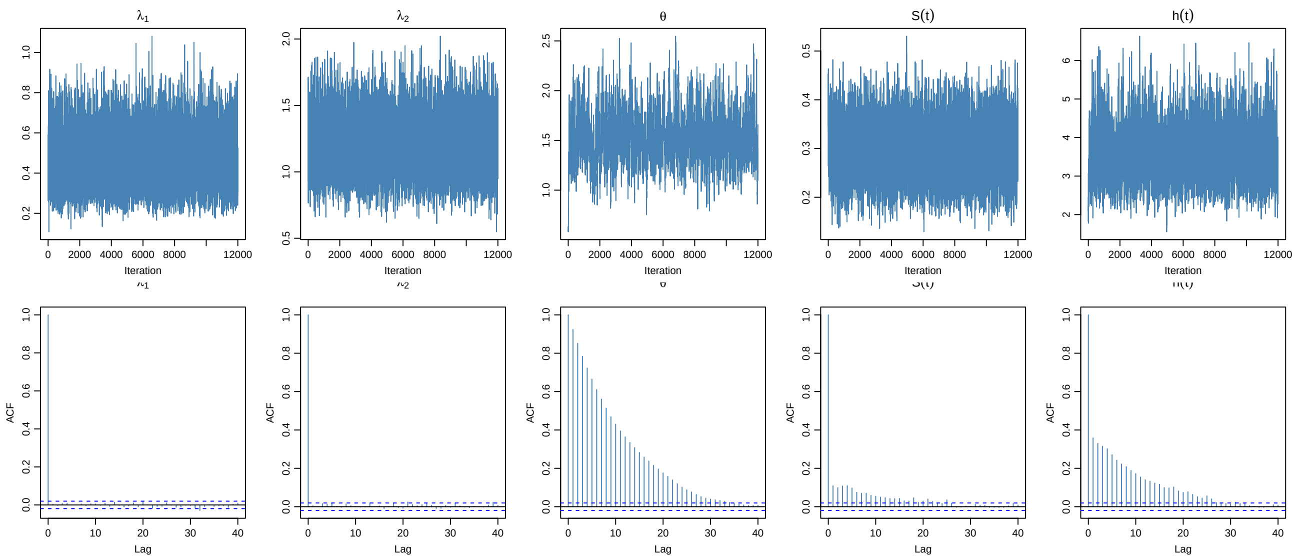

Figure 2. Trace plots (top row) and ACF plots (bottom row) for the posterior draws of λ_1, λ_2, θ, $S(t_0)$, and $h(t_0)$ under the representative setting $(n, m) = (40, 20)$, Scheme U, $(T_1, T_2) = (0.4, 0.8)$, $M = 12{,}000$, and burn-in = 2,000.

The trace plots fluctuate around stable levels without systematic trends, confirming the satisfactory convergence of all five chains. The ACF plots confirm rapid decay for λ_1 and λ_2 (sampled via exact Gibbs draws) and moderate decay for θ (sampled via MH). This contrast is the key visual confirmation of the hybrid sampler advantage: The scale parameter chains are effectively uncorrelated after a few lags, while the shape parameter chain retains moderate autocorrelation, reflecting the single MH step per iteration.

Table 4 reports the posterior means, standard deviations, and ESS values for the representative run.

Table 4. Posterior summaries and Markov chain Monte Carlo (MCMC) diagnostics for the representative run: $(n, m) = (40, 20)$, Scheme U, $(T_1, T_2) = (0.4, 0.8)$, $M = 12{,}000$, burn-in $= 2{,}000$, and Prior II. True values: $\theta = 1.5$, $\lambda_1 = 0.5$, $\lambda_2 = 1.0$, $S(t_0) = 0.3273$, $h(t_0) = 3.1755$, $\pi_1 = 0.3333$.

Parameter	True	Post. Mean	Post. SD	ESS	Acceptance (θ)
θ	1.5000	1.5191	0.2639	333.3	0.8613
λ_1	0.5000	0.4631	0.1248	2079.5	—
λ_2	1.0000	1.1941	0.1977	1915.7	—
$S(t_0)$	0.3273	0.2935	0.0537	1464.6	—
$h(t_0)$	3.1755	3.5640	0.6486	741.1	—
π_1	0.3333	0.2793	0.0629	1924.7	—

Table 5. MCMC diagnostics: Average MH acceptance rate for θ, and average ESS across $G = 1{,}000$ replications per scenario.

(T_1, T_2)	(n, m)	Scheme	Accept. θ	ESS θ	ESS λ_1	ESS λ_2	Ratio $\frac{\mathrm{ESS}_{\lambda_1}}{\mathrm{ESS}_\theta}$
(0.4, 0.8)	$(40, 20)$	U	0.8549	272.6	1992.9	1921.3	7.3
		L	0.8497	281.5	1958.1	1848.1	7.0
		M	0.8531	279.5	2001.9	1916.5	7.2
		R	0.8581	268.2	2013.4	1973.4	7.5
	$(40, 30)$	U	0.8439	290.0	1876.6	1703.2	6.5
		L	0.8432	291.1	1863.4	1680.0	6.4
		M	0.8461	287.0	1901.3	1735.5	6.6
		R	0.8489	280.2	1904.5	1739.9	6.8
	$(80, 40)$	U	0.8479	280.8	1882.4	1703.4	6.7
		L	0.8373	298.2	1774.4	1545.1	6.0
		M	0.8445	288.4	1887.2	1704.5	6.5
		R	0.8545	270.5	1944.4	1826.3	7.2
	$(80, 60)$	U	0.8276	304.6	1650.0	1356.2	5.4
		L	0.8258	306.5	1624.7	1318.3	5.3
		M	0.8314	300.0	1693.8	1409.0	5.6
		R	0.8365	290.3	1685.4	1393.4	5.8
(0.8, 1.5)	$(40, 20)$	U	0.8543	273.8	1990.3	1915.4	7.3
		L	0.8432	293.5	1906.0	1756.9	6.5
		M	0.8491	288.1	1964.2	1863.3	6.8
		R	0.8578	266.9	2017.1	1974.2	7.6
	$(40, 30)$	U	0.8349	304.0	1814.6	1591.0	6.0
		L	0.8334	304.1	1791.9	1564.3	5.9
		M	0.8384	299.3	1847.6	1655.9	6.2
		R	0.8489	279.1	1899.7	1745.7	6.8
	$(80, 40)$	U	0.8463	284.4	1874.0	1698.2	6.6
		L	0.8246	313.7	1702.4	1420.1	5.4
		M	0.8355	303.7	1824.7	1616.0	6.0
		R	0.8547	270.5	1948.9	1825.7	7.2
	$(80, 60)$	U	0.8101	326.1	1563.8	1241.0	4.8
		L	0.8073	329.7	1526.9	1208.6	4.6
		M	0.8163	323.6	1623.6	1321.2	5.0
		R	0.8365	289.6	1684.9	1386.9	5.8

The ESS values confirm the computational advantage of the hybrid Gibbs–MH algorithm quantitatively: The ESS values for λ_1 (2,079.5) and λ_2 (1,915.7) are 6–7 times larger than the ESS for θ (333.3), demonstrating that the exact Gibbs draws achieve near-perfect mixing for the scale parameters, while only θ is constrained by the MH autocorrelation. The log-scale random walk proposal for θ uses a fixed step size of $s_\theta = 0.08$, which produces MH acceptance rates in the range 0.81–0.86 across all 32 scenarios (Table 5). These rates lie above the conventional 20%–40% target for random walk proposals [15], indicating that this step size is smaller than optimal and yields a moderately autocorrelated θ chain, with ESS values ranging from approximately 267 to 333 across the simulation scenarios. To quantify this and identify a better mixing setting, we conducted a dedicated proposal-scale study, reported in Section 6.6. The point and interval estimates in Tables S1–S10 depend only on the target posterior and are therefore invariant to s_θ; the proposal scale affects Monte Carlo efficiency alone.

As an additional convergence check, four parallel chains were run from over-dispersed starting values for the representative design. For the three model parameters, the Gelman–Rubin potential scale reduction factors were essentially equal to one ($\widehat{R} \leq 1.002$), and the Monte Carlo standard errors ranged from 0.00137 to 0.00857, all below 0.01 and small relative to the corresponding posterior standard deviations, further confirming satisfactory convergence and adequate mixing of the hybrid Gibbs–Metropolis–Hastings sampler.

6.4. Point estimation results

Tables S1–S6 report the average estimates $\bar{\hat{\psi}}$, RMSE, and MRAB for θ, λ_1, λ_2, $S(t_0)$, $h(t_0)$, and π_1 across all 32 scenarios. Point estimation entries are formatted as $\bar{\hat{\psi}}$ (RMSE, MRAB).

The simulation results reveal three consistent patterns. First, the accuracy of estimation depends strongly on the censoring scheme: The right-heavy scheme R generally produces the largest RMSE and MRAB values, particularly for θ and $h(t_0)$, because fewer late failures are observed, whereas the balanced and left-heavy schemes provide more stable estimations. Second, the superiority of Bayes II is most pronounced under heavy censoring, where the moderately informative prior regularizes the estimation of θ and consequently improves the estimation of $S(t_0)$ and $h(t_0)$. Because Prior II is centered at the true parameter values, these gains should be interpreted as a best-case benchmark; their dependence on the prior specification is examined in the sensitivity analysis of Section 6.7. Finally, the interval estimation results in Section 6.5 show that the main difficulty lies in calibration rather than numerical singularity: The delta method ACIs tend to undercover for θ and become excessively wide for $h(t_0)$ under heavy right-censoring, whereas the Bayesian HPD intervals remain shorter and better calibrated.

6.5. Interval estimation results

Tables S7–S10 report the ACL and CP for all parameters. Interval entries are formatted as ACLs (CPs). Across all 32 scenarios and $G = 1000$ replications, the observed Fisher information matrix was invertible in every replication in which the MLE converged (optimization failed in a single replication out of 32,000), and fewer than 2% of replications produced a non-finite or non-positive variance estimate (at most 1.8%, occurring under the right-heavy Scheme R, with all other configurations below 1.3%). Delta method ACIs are therefore reported for all six quantities, although their finite-sample behavior differs markedly by parameter. For the shape parameter θ, the ACIs undercover substantially under heavy and right-heavy censoring, with empirical coverage falling to approximately 0.81 under Scheme R when $(n, m) = (40, 20)$, and remaining below 0.86 under Scheme R even at $(n, m) = (80, 40)$. For the hazard rate $h(t_0)$, the ACIs achieve near-nominal coverage only through excessively wide intervals, with average lengths reaching approximately 20 under right-heavy schemes. The ACIs for λ_1 and λ_2 are better behaved but exhibit mild undercoverage, whereas those for $S(t_0)$ and π_1 remain well calibrated, with coverage close to the nominal 0.95 throughout. In all scenarios, the Bayesian HPD intervals under Prior II are considerably shorter while maintaining coverage at or above the nominal level, and are therefore the recommended basis for interval inference on θ and $h(t_0)$.

6.6. *Proposal-scale study for the MH step*

Only the shape parameter θ is updated by a random walk MH step; the scale parameters λ_1 and λ_2 have exact Gamma full conditionals and are drawn by Gibbs sampling, so their chains are effectively independent (ESS $\approx$ 2,000 throughout) and the acceptance rate concerns the single θ block alone. Because the fixed step size $s_\theta = 0.08$ used above yields acceptance rates of 0.81–0.86, which are above the recommended band, we examined the effect of the proposal scale on both the acceptance rate and the ESS. For the representative design $(n, m) = (40, 20)$, scheme U, $(T_1, T_2) = (0.4, 0.8)$ and Prior II, we varied the log-scale random walk standard deviation s_θ over $\{0.05, 0.08, 0.15, 0.30, 0.60, 1.00\}$; the results are summarized in Table 6.

Table 6. Effect of the random walk proposal scale s_θ on the MH acceptance rate and ESS, for $(n, m) = (40, 20)$, Scheme U, $(T_1, T_2) = (0.4, 0.8)$, Prior II. ESS_{λ_1} is reported for reference; λ_1 is Gibbs-sampled and hence near-independent.

s_θ	Acceptance rate	ESS_θ	ESS_{λ_1}
0.05	0.908	143.0	1921.3
0.08	0.855	270.0	1984.3
0.15	0.739	567.2	2028.9
0.30	0.547	915.0	2047.2
0.60	0.333	921.0	2048.6
1.00	0.213	720.9	2032.6

The results confirm the expected trade-off. At the small scales that produce the high acceptance rates reported above (s_θ = 0.05–0.08, acceptance 0.91–0.85), the ESS for θ is low (ESS_θ = 143–270), reflecting strong autocorrelation. As s_θ increases, the acceptance rate falls into the recommended band and ESS_θ rises sharply, peaking at 915–921 for s_θ = 0.30–0.60, where the acceptance rate is 0.55 and 0.33, respectively; beyond this ($s_\theta = 1.00$), too many proposals are rejected and ESS_θ declines to 721. Throughout, $\mathrm{ESS}_{\lambda_1} \approx$ 2,000, confirming that the Gibbs-sampled scale parameters mix essentially independently of the proposal scale. The proposal-scale study suggests that values around $s_\theta \approx 0.30$ provide improved mixing efficiency, increasing ESS_θ by approximately a factor of three relative to $s_\theta = 0.08$, while leaving the posterior summaries essentially unchanged. Since the proposal scale affects only the Monte Carlo efficiency and not the target posterior, the point and interval estimates reported in Sections 6.4 and 6.5 are unchanged; we verified this on the representative scenario, where re-running at $s_\theta = 0.30$ left the posterior means and HPD coverages unchanged to within Monte Carlo error.

Averaged over 200 independently generated datasets, the hybrid Gibbs–Metropolis sampler and a fully MH implementation achieved identical θ acceptance rates (0.855 versus 0.855, since both use the same random walk update for θ), but the exact Gamma draws for λ_1, λ_2 in the hybrid scheme yielded substantially higher ESSs for the scale parameters ($\mathrm{ESS}_{\lambda_1} = 1975.0$ versus 384.9 and $\mathrm{ESS}_{\lambda_2} = 1918.5$ versus 546.3) at a lower cost (0.514s versus 0.974s per run). In this representative comparison, the hybrid sampler therefore delivered about 9.7 times the effective samples per second for λ_1 (3842.4 versus 395.2), while the posterior summaries agreed to within Monte Carlo error.

6.7. Sensitivity to prior specification

The strong performance of Prior II documented above is obtained under a prior whose mean coincides with the true parameter values. To assess how the Bayesian estimators behave when this information is inaccurate, we repeat the study for the two representative designs $(n, m) = (40, 20)$ and $(80, 40)$ under the uniform (U) and right-heavy (R) schemes with $(T_1, T_2) = (0.4, 0.8)$, using four Gamma priors. Prior II is the centered baseline. Priors III and IV are deliberately location-misspecified: Their means are set to +100% and −50% of the true values, respectively, obtained by rescaling the rate hyperparameters while keeping the shape hyperparameters fixed. Prior V is correctly centered but diffuse, with coefficients of variation $1/\sqrt{a}$ (shape parameters $a = 1, 2, 3$ for $\lambda_1, \lambda_2, \theta$), namely 1.00, 0.71 and 0.58. The four priors are as follows, in the $(\lambda_1, \lambda_2, \theta)$ ordering of the hyperparameters:

Prior II (centered): $\lambda_1 \sim \Gamma(10, 20)$, $\lambda_2 \sim \Gamma(20, 20)$, $\theta \sim \Gamma(30, 20)$; means $(0.5, 1.0, 1.5)$.

Prior III (+100%): $\lambda_1 \sim \Gamma(10, 10)$, $\lambda_2 \sim \Gamma(20, 10)$, $\theta \sim \Gamma(30, 10)$; means $(1.0, 2.0, 3.0)$.

Prior IV (−50%): $\lambda_1 \sim \Gamma(10, 40)$, $\lambda_2 \sim \Gamma(20, 40)$, $\theta \sim \Gamma(30, 40)$; means $(0.25, 0.5, 0.75)$.

Prior V (diffuse, centered; CV = 1.00, 0.71, 0.58): $\lambda_1 \sim \Gamma(1, 2)$, $\lambda_2 \sim \Gamma(2, 2)$, $\theta \sim \Gamma(3, 2)$; means $(0.5, 1.0, 1.5)$.

Table 7 reports the posterior mean and the empirical 95% HPD CP for each quantity. Three findings stand out. First, the quality of the Bayesian estimator is governed by the location of the prior rather than its concentration: Under the badly mis-centered Priors III and IV, the posterior means are pulled toward the prior mean and the coverage for the shape parameter θ. For the derived survival and hazard functions, it collapses far below the nominal level (for $(40, 20)$-U, the CP of θ falls from 1.00 under Prior II to 0.25 under Prior III and 0.00 under Prior IV). Second, a prior that is merely correctly scaled but otherwise vague (Prior V) recovers essentially the baseline behavior, with near-nominal coverage and only modestly wider intervals, showing that an unrealistically precise prior is not required. Third, increasing the sample size mitigates but does not remove the effect of a mis-centered prior (the CP of θ under Prior III rises only from 0.25 to 0.42 as (n, m) grows from $(40, 20)$ to $(80, 40)$), whereas the relative risk π_1 is estimated robustly under every prior, as it is directly identified by the data. In practice, we therefore recommend the weakly informative Prior I or a correctly scaled diffuse prior of the Prior V type whenever reliable historical information is unavailable, and we reserve strongly informative priors for settings supported by genuine prior data.

Table 7. Prior sensitivity analysis: Posterior mean and 95% highest posterior density (HPD) coverage (Mean (CP)) under four Gamma priors. Prior II is centered at the truth; Priors III and IV mislocate the mean by +100% and −50%; Prior V is centered but diffuse (coefficient of variation (CV) = $1/\sqrt{a}$, $a = 1, 2, 3$). $(T_1, T_2) = (0.4, 0.8)$, M = 12,000, burn-in = 2,000, G = 1,000. True values: $\theta = 1.5$, $\lambda_1 = 0.5$, $\lambda_2 = 1.0$, $S(t_0) = 0.3273$, $h(t_0) = 3.1755$, $\pi_1 = 0.3333$.

(n, m)	Sch	Prior	θ	λ_1	λ_2	$S(t_0)$	$h(t_0)$	π_1
(40, 20)	U	II	1.510 (1.000)	0.501 (0.995)	1.014 (0.995)	0.328 (0.996)	3.250 (0.995)	0.331 (0.996)
		III	2.337 (0.250)	0.648 (0.956)	1.313 (0.827)	0.168 (0.121)	6.480 (0.098)	0.331 (0.998)
		IV	0.797 (0.000)	0.323 (0.350)	0.653 (0.028)	0.551 (0.000)	1.456 (0.000)	0.331 (1.000)
		V	1.569 (0.999)	0.512 (0.947)	1.051 (0.973)	0.324 (0.957)	3.537 (0.982)	0.327 (0.909)
	R	II	1.507 (1.000)	0.501 (0.996)	1.012 (0.996)	0.329 (0.997)	3.242 (0.997)	0.331 (0.998)
		III	2.517 (0.073)	0.655 (0.955)	1.323 (0.815)	0.152 (0.083)	7.188 (0.069)	0.331 (0.997)
		IV	0.782 (0.000)	0.321 (0.328)	0.647 (0.018)	0.555 (0.000)	1.434 (0.000)	0.331 (0.997)
		V	1.568 (1.000)	0.512 (0.937)	1.043 (0.969)	0.325 (0.957)	3.604 (0.988)	0.329 (0.912)
(80, 40)	U	II	1.508 (1.000)	0.504 (0.992)	1.002 (0.993)	0.329 (0.994)	3.220 (0.993)	0.335 (0.986)
		III	2.179 (0.419)	0.573 (0.973)	1.140 (0.969)	0.220 (0.296)	5.166 (0.224)	0.335 (0.986)
		IV	0.831 (0.000)	0.372 (0.648)	0.740 (0.280)	0.504 (0.000)	1.688 (0.000)	0.335 (0.986)
		V	1.533 (0.990)	0.512 (0.948)	1.015 (0.971)	0.328 (0.967)	3.345 (0.983)	0.335 (0.928)
	R	II	1.507 (1.000)	0.502 (0.992)	1.004 (0.990)	0.329 (0.994)	3.224 (0.997)	0.333 (0.987)
		III	2.395 (0.143)	0.574 (0.983)	1.148 (0.937)	0.199 (0.204)	5.817 (0.147)	0.333 (0.987)
		IV	0.803 (0.000)	0.367 (0.589)	0.733 (0.243)	0.510 (0.000)	1.647 (0.000)	0.333 (0.987)
		V	1.563 (0.998)	0.506 (0.958)	1.013 (0.970)	0.327 (0.973)	3.455 (0.987)	0.333 (0.935)

7. Real data applications

7.1. Dataset description

To illustrate the practical performance of the proposed Gompertz competing risks model under IAT-II PCS, we apply the methodology to the electrode voltage–endurance dataset originally reported by [29] and subsequently analyzed under Weibull competing risks frameworks by [14]. The dataset records the lifetimes, measured in thousands of hours, of $n = 58$ electrical insulation electrodes subjected to a constant high-voltage stress test.

Two physically distinct failure mechanisms were identified. Cause 1 (Mode E) refers to failure due to electrical breakdown of the insulation material, associated with dielectric degradation accelerated by the applied voltage. Cause 2 (Mode D) refers to failure due to surface discharge and electrode erosion, driven by partial discharge activity at the electrode's surface. Observations for which the unit was removed from the test before failure are classified as right-censored and denoted by (+) in Table 8. Of the 58 units, 19 failed from Cause 1, 26 failed from Cause 2, and 13 were right-censored. The observed failure times span the range of $[0.002, 0.446]$ thousand hours. The dataset exhibits two actively competing failure modes with different distributional characteristics, making it a suitable benchmark dataset for competing risks analysis.

Figure 3 presents a histogram of the failure times by cause and a dot plot of all observed times. Cause 2 (Mode D) failures are concentrated in the upper half of the time range ($\approx$ 0.168–0.446 thousand hours), whereas Cause 1 (Mode E) failures are spread more uniformly, with several early failures before 0.10 thousand hours. This pattern is consistent with two distinct failure mechanisms having different acceleration characteristics.

Table 8. Voltage-endurance life-test results (in thousands of hours) for $n = 58$ electrodes. E = Mode E (Cause 1); D = Mode D (Cause 2); + = right-censored. Source: [29].

Time ($\times 10^3$ h)	Mode	Time ($\times 10^3$ h)	Mode
0.002	E	0.226	E
0.003	E	0.236	E
0.005	E	0.241	+
0.008	E	0.257	+
0.013	+	0.261	D
0.021	E	0.264	D
0.028	E	0.278	D
0.031	E	0.282	E
0.031	+	0.284	D
0.052	+	0.286	D
0.053	+	0.298	D
0.064	E	0.303	E
0.067	+	0.314	D
0.069	E	0.317	D
0.076	E	0.318	D
0.078	+	0.320	D
0.104	E	0.327	D
0.113	+	0.328	D
0.119	E	0.328	D
0.135	+	0.348	D
0.144	E	0.348	+
0.157	+	0.350	D
0.160	E	0.360	D
0.168	D	0.369	D
0.179	+	0.377	D
0.191	D	0.387	D
0.203	D	0.392	D
0.211	D	0.412	D
0.221	E	0.446	D

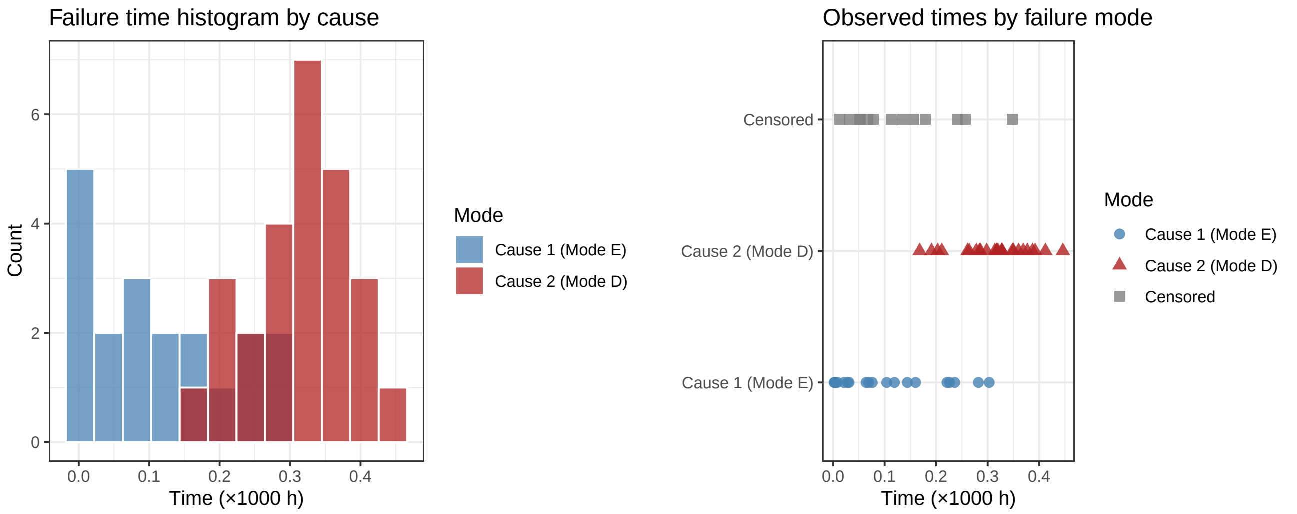

Figure 3. Observed electrode lifetimes by failure mode. Left: Histogram of failure times for Mode E (Cause 1) and Mode D (Cause 2). Right: Dot plot of all 58 observed times by mode and censoring status.

7.2. *Goodness-of-fit assessment*

Before applying the proposed IAT-II PCS framework, we assess the adequacy of the Gompertz distribution for each failure mode by fitting separate two-parameter models to the uncensored failure times from Cause 1 ($n_1 = 19$) and Cause 2 ($n_2 = 26$). The Weibull distribution is included as a benchmark. Since the parameters are estimated from the same data used for testing, the nominal Kolmogorov–Smirnov (KS) p-values are anti-conservative; a parametric bootstrap procedure with $B = 500$ replicates is therefore used to obtain valid p-values, following the recommendation of [30].

Table 9. Marginal descriptive goodness-of-fit comparison of the observed cause-specific failure times: Gompertz, Weibull, exponential, and log-logistic distributions fitted separately to each cause. Lower AIC/BIC and larger bootstrap p-values indicate a better fit.

Cause	Model	n	Shape	Scale	LogLik	AIC	BIC	KS	p_{boot}
Cause 1	Gompertz	19	2.0298	7.3098	23.0618	−42.1236	−40.2347	0.1599	0.200
	Weibull	19	0.8888	7.3987	23.0256	−42.0512	−40.1624	0.1186	0.716
	Exponential	19	—	0.1106	22.8294	−43.6589	−42.7144	0.1408	0.636
	Log-logistic	19	1.1176	0.0628	20.4988	−36.9977	−35.1088	0.1469	0.200
Cause 2	Gompertz	26	16.2909	0.0590	32.9780	−61.9559	−59.4397	0.1242	0.340
	Weibull	26	5.4140	346.3466	33.6209	−63.2418	−60.7256	0.0957	0.760
	Exponential	26	—	0.3130	4.2035	−6.4071	−5.1490	0.4183	0.000
	Log-logistic	26	7.6697	0.3128	31.6433	−59.2865	−56.7703	0.1228	0.272

The results in Table 9 reveal an important asymmetry between the two failure modes. For Cause 1 (Mode E), both the Gompertz and Weibull distributions provide an adequate fit. The Gompertz model achieves a log-likelihood of 23.0618 (AIC = −42.1236, p_{boot} = 0.200), and the Weibull model performs comparably (log-likelihood = 23.0256, AIC = −42.0512, p_{boot} = 0.716). Thus, both models are statistically acceptable for Cause 1.

For Cause 2 (Mode D), a markedly different picture emerges. The Weibull distribution provides an excellent fit (p_{boot} = 0.760, AIC = −63.2418), whereas the Gompertz model yields a lower log-likelihood (32.9780 versus 33.6209) and a weaker bootstrap p-value of 0.340. The estimated Gompertz shape parameter $\hat{\theta} = 16.2909$ corresponds to a sharply increasing exponential hazard rate that is not fully consistent with the empirical failure pattern of Mode D. By contrast, the Weibull estimate $\hat{\alpha} = 5.414$ suggests a power-law increasing hazard, providing a more physically plausible description of the erosion-driven failure mechanism. These goodness-of-fit results are consistent with findings reported for the Nadarajah–Haghighi distribution by [3], who also documented boundary behavior and poor fit for Mode D. The present analysis suggests that Cause 2 failures follow a Weibull-type degradation process more closely than a Gompertz-type process, while Cause 1 is described adequately by both distributions. This finding motivates the model comparison in Section 7.6.

To broaden the marginal goodness-of-fit assessment, the exponential and log-logistic distributions were also fitted separately to the observed failure times from each cause. The comparison indicates that no single distribution is uniformly superior for both failure modes. The exponential model provides an adequate fit for Cause 1, whereas it performs poorly for Cause 2. The log-logistic model provides a reasonable fit in some settings but does not offer a uniformly better fit than the Gompertz and Weibull alternatives. Overall, the Gompertz model provides a satisfactory and comparatively balanced description of the two failure modes, while the joint IAT-II PCS comparison continues to favor the Gompertz formulation over the Weibull alternative.

As a graphical complement to the numerical goodness-of-fit statistics, Figure 4 presents probability–probability (P–P) plots of the fitted Gompertz and Weibull models for each failure cause. The plotted points lie reasonably close to the diagonal for both causes, providing additional support for the adequacy of the two fitted models.

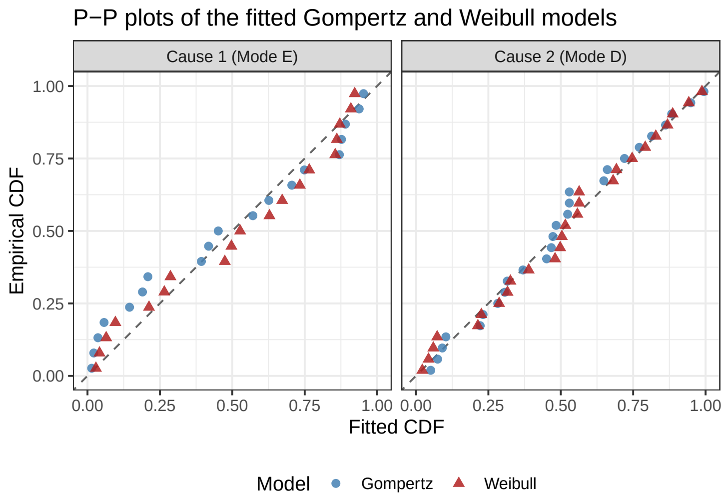

Figure 4. Probability–probability (P–P) plots of the fitted Gompertz and Weibull distributions for the observed failure times of each cause. Points close to the diagonal indicate a good fit.

7.3. Generation of IAT-II PCS scenarios

Three censored scenarios are generated from the original electrode dataset using different threshold configurations. The $n = 45$ observed failure times with identified causes are treated as the complete population, and the IAT-II PCS algorithm of Section 3 is applied with a uniform censoring scheme (Scheme U). The resulting scenarios are summarized in Table 10.

Table 10. IAT-II PCS scenarios generated from the electrode voltage–endurance dataset ($n = 45$ observed failures used as the population). E_2: Effective sample size; D_1, D_2: Cause-specific observed failures; T^*: Termination time; B: Units withdrawn at T^*.

Scenario	n	m	Case	E_2	D_1	D_2	T_1	T_2	T^*	B	Scheme
Scenario 1	45	25	I	25	14	11	0.42	0.50	0.387	0	U
Scenario 2	45	25	II	25	15	10	0.23	0.38	0.328	5	U
Scenario 3	45	22	III	21	15	6	0.18	0.30	0.300	10	U

The three scenarios represent all three censoring cases of the IAT-II PCS. Case I has $X_{m:m:n} < T_1 = 0.42$: All $m = 25$ failures occur before the lower threshold, the experiment terminates at $T^* = 0.387$, and $B = 0$. Case II has $T_1 \leq X_{m:m:n} \leq T_2$: The mth failure falls in $[T_1, T_2] = [0.23, 0.38]$, the experiment terminates at $T^* = 0.328$, and $B = 5$ units are withdrawn. Case III has $X_{m:m:n} > T_2 = 0.30$: The experiment is terminated at $T^* = T_2 = 0.300$ with only $k_2 = 21$ failures observed and $B = 10$ simultaneous withdrawals. Together, the three scenarios provide a comprehensive evaluation of the inferential framework across all three censoring regimes.

7.4. Profile log-likelihood analysis

Figure 5 presents the profile log-likelihood functions of θ, computed for each of the three IAT-II PCS scenarios by substituting the closed-form expressions $\hat{\lambda}_j(\theta) = D_j\,\theta/W(\theta)$ (Eq (4.3)) into the log-likelihood (3.2).

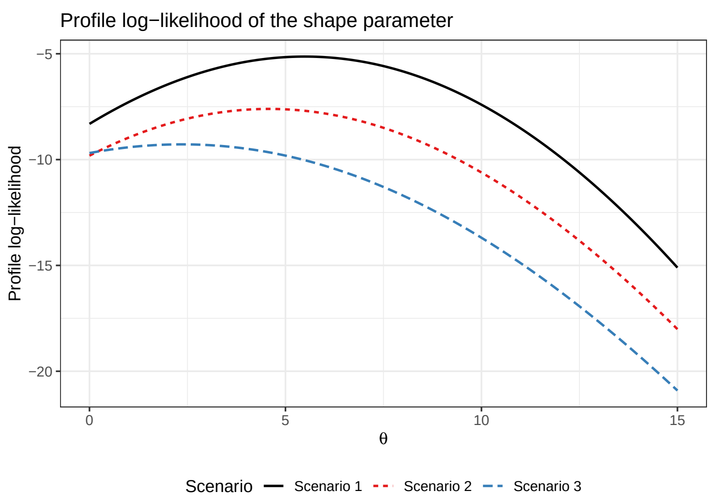

Figure 5. Profile log-likelihood functions of θ for the three IAT-II PCS electrode scenarios, computed using $\hat{\lambda}_j(\theta) = D_j\,\theta/W(\theta)$.

The profile log-likelihood curves are well behaved and possess clear interior maxima for all three scenarios, confirming that θ is identifiable from each censored scenario. The profile MLE values ($\hat{\theta} = 5.49,\ 4.58,\ 2.36$ for Scenarios 1, 2, and 3, respectively) are relatively large, consistent with the exponentially increasing hazard of the Gompertz distribution capturing the accelerating failure rate in the electrode data. The moderate curvature around the maxima reflects the limited Fisher information in the censored scenarios, which motivates the use of the Bayesian framework to stabilize inference for θ through the incorporation of prior information.

7.5. Point and interval estimation

Table 11 reports the MLEs and 95% ACIs from the observed Fisher information matrix, together with the Bayesian posterior means, posterior standard deviations, 95% HPD credible intervals, and ESSs for all parameters and reliability characteristics at mission time $t_0 = 0.5$ thousand hours. Bayesian estimates are computed under the moderately informative Prior II ($a_1 = 10,\ b_1 = 20,\ a_2 = 20,\ b_2 = 20,\ a_3 = 30,\ b_3 = 20$). The MH acceptance rate for θ was approximately 0.86 across all scenarios.

Several important observations emerge from Table 11. First, the MLEs of θ are large (5.49, 4.58, and 2.36) and their ACIs exhibit one-sided instability, reflecting boundary behavior of the Gompertz shape parameter under the censored electrode scenarios. Second, the Bayesian posterior means of θ are more stable and consistent across the three scenarios (1.671, 1.647, and 1.604), indicating that the moderately informative prior effectively regularizes estimation of the shape parameter. Third, the posterior means of $S(t_0)$ range from 0.220 to 0.255 with HPD interval widths of approximately 0.19–0.21, indicating stable reliability estimates across all three censoring configurations. Fourth, the ESS values for λ_1 and λ_2 ($\approx$ 2,000–2,230) are substantially larger than those for θ ($\approx$ 225–327), by a factor of approximately 6–8, confirming the computational advantage of the hybrid Gibbs–MH algorithm: The exact Gibbs draws for the scale parameters achieve substantially improved mixing and sampling efficiency, while only θ requires MH updates. Fifth, the posterior means of the relative risk $\pi_1 = P(X_1 < X_2)$ range from 0.436 to 0.490 across the three scenarios, indicating that the two failure modes contribute roughly equally to the overall failure process, with Cause 2 (Mode D) being marginally more likely to be the operative failure mode in each censoring configuration.

Figure 6 presents the posterior density and trace plots for all parameters under Scenario 1. The posterior densities of λ_1 and λ_2 are approximately symmetric and unimodal, indicating well-identified scale parameters. The posterior of θ is slightly right-skewed, reflecting its boundary tendency. The trace plots confirm satisfactory convergence of the hybrid Gibbs–MH sampler, with the θ chain showing higher autocorrelation relative to λ_1 and λ_2, consistent with the ESS values in Table 11. Figures 7 and 8 display the corresponding posterior density and trace plots under Scenarios 2 and 3, respectively, and confirm the same convergence behavior across the remaining censoring cases.

Table 11. Point and interval estimation results for the electrode dataset under the Gompertz competing risks model (t_0 = 0.5 thousand hours, M = 12,000, burn-in = 2,000, Prior II). ACI: 95% asymptotic confidence interval (delta method); HPD: 95% highest posterior density interval; ESS: effective sample size. '—' denotes a numerically unstable upper bound due to boundary behavior of the MLE for θ.

Scenario	Par.	MLE	95% ACI	Bayes Mean	Bayes SD	95% HPD	ESS
Scenario 1	θ	5.4921	(1.3246, —)	1.6712	0.2934	(1.1399, 2.2551)	225.6
	λ_1	1.0065	(0.1436, —)	0.8570	0.1749	(0.5342, 1.2053)	2139.6
	λ_2	0.7908	(0.0792, —)	1.1100	0.2003	(0.7227, 1.5055)	2050.4
	$S(t_0)$	0.0085	(0.0000, 0.0441)	0.2198	0.0506	(0.1216, 0.3181)	861.1
	$h(t_0)$	28.0047	(0.0000, —)	4.5777	0.8886	(2.9623, 6.3828)	429.7
	π_1	0.5600	(0.3654, 0.7546)	0.4357	0.0661	(0.3019, 0.5590)	2230.1
Scenario 2	θ	4.5790	(0.3213, —)	1.6466	0.2902	(1.0947, 2.2047)	327.4
	λ_1	1.1052	(0.1463, —)	0.8727	0.1751	(0.5494, 1.2233)	2029.6
	λ_2	0.7368	(0.0453, —)	1.0468	0.1903	(0.6849, 1.4189)	2103.4
	$S(t_0)$	0.0282	(0.0000, 0.1120)	0.2300	0.0502	(0.1328, 0.3269)	1118.1
	$h(t_0)$	18.1803	(0.0000, —)	4.4098	0.8437	(2.8708, 6.0427)	595.8
	π_1	0.6000	(0.4080, 0.7920)	0.4546	0.0661	(0.3250, 0.5837)	2101.3
Scenario 3	θ	2.3581	(0.0000, —)	1.6043	0.2805	(1.0762, 2.1443)	298.6
	λ_1	1.6514	(0.2493, —)	0.8834	0.1751	(0.5543, 1.2304)	2177.5
	λ_2	0.6606	(0.0000, —)	0.9215	0.1818	(0.5764, 1.2728)	2001.9
	$S(t_0)$	0.1100	(0.0000, 0.3354)	0.2552	0.0532	(0.1536, 0.3608)	1178.0
	$h(t_0)$	7.5171	(0.0000, —)	4.0586	0.7799	(2.6828, 5.6614)	600.4
	π_1	0.7143	(0.5211, 0.9075)	0.4896	0.0694	(0.3545, 0.6231)	2209.7

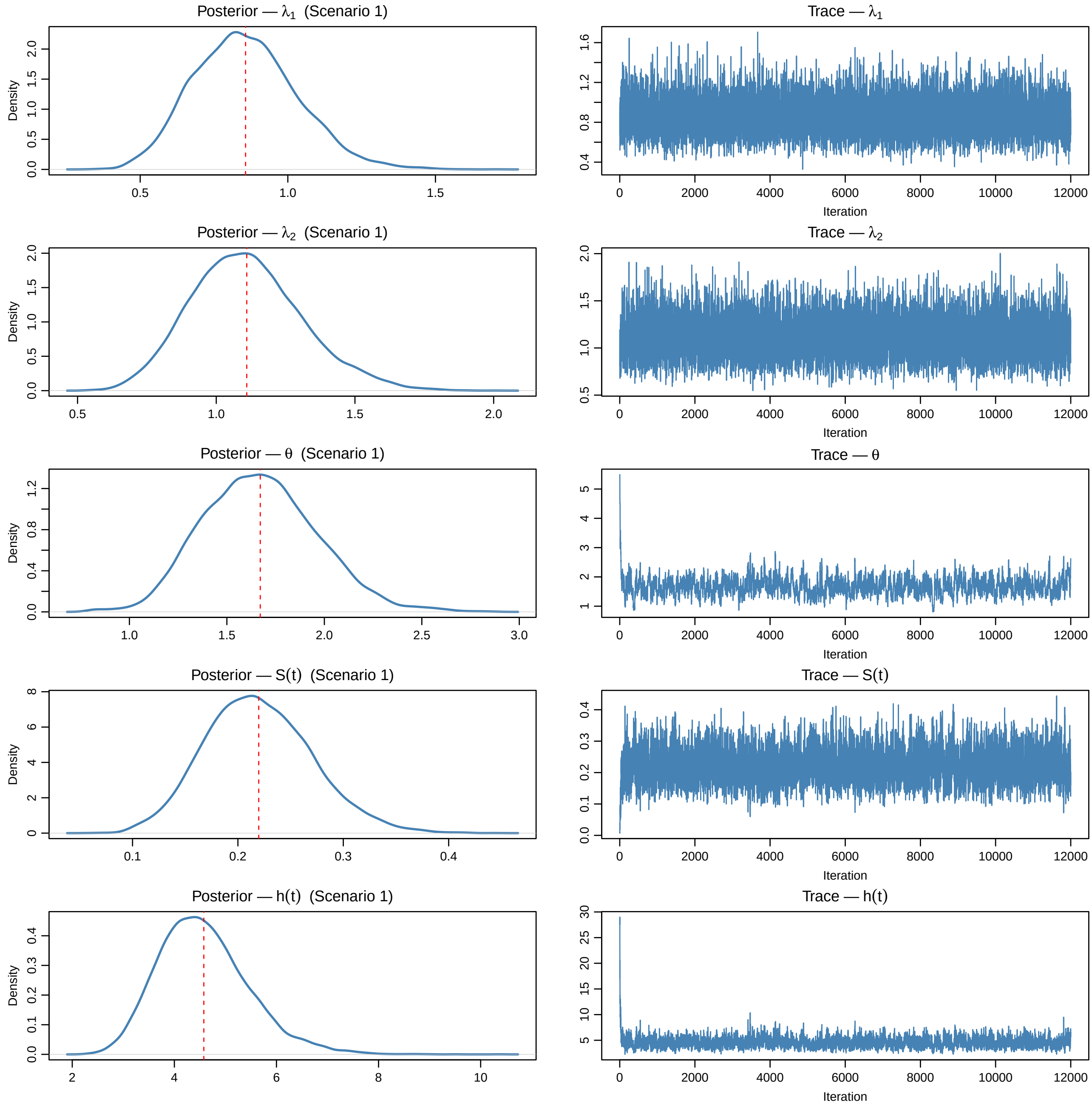

Figure 6. Posterior density plots (left column) and trace plots (right column) for θ, λ_1, λ_2, $S(t_0)$, and $h(t_0)$ under Scenario 1 (M = 12,000, burn-in = 2,000, Prior II). The red dashed line marks the posterior mean.

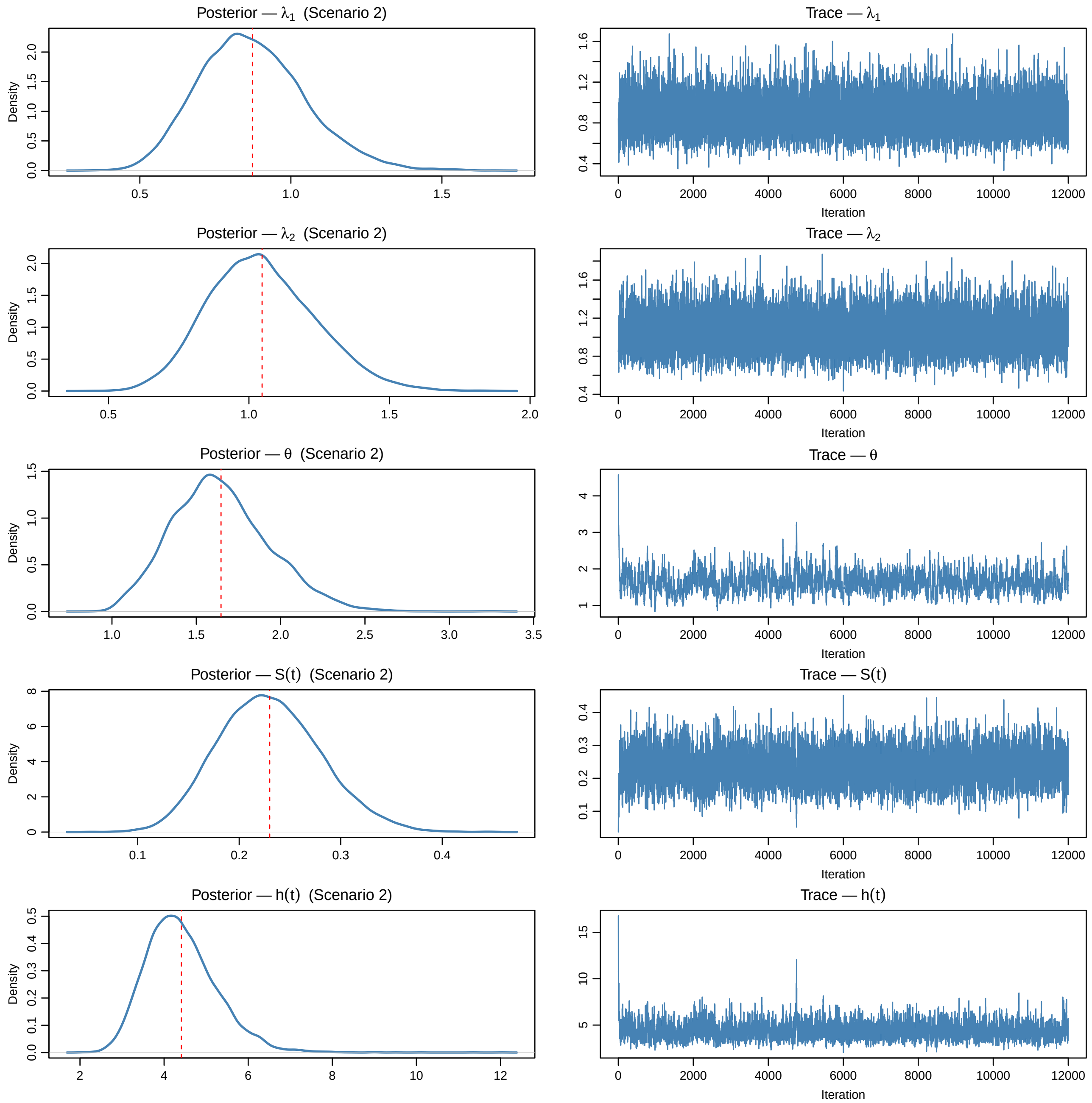

Figure 7. Posterior density plots (left column) and trace plots (right column) for θ, λ_1, λ_2, $S(t_0)$, and $h(t_0)$ under Scenario 2 ($M = 12{,}000$, burn-in $= 2{,}000$, Prior II). The red dashed line marks the posterior mean.

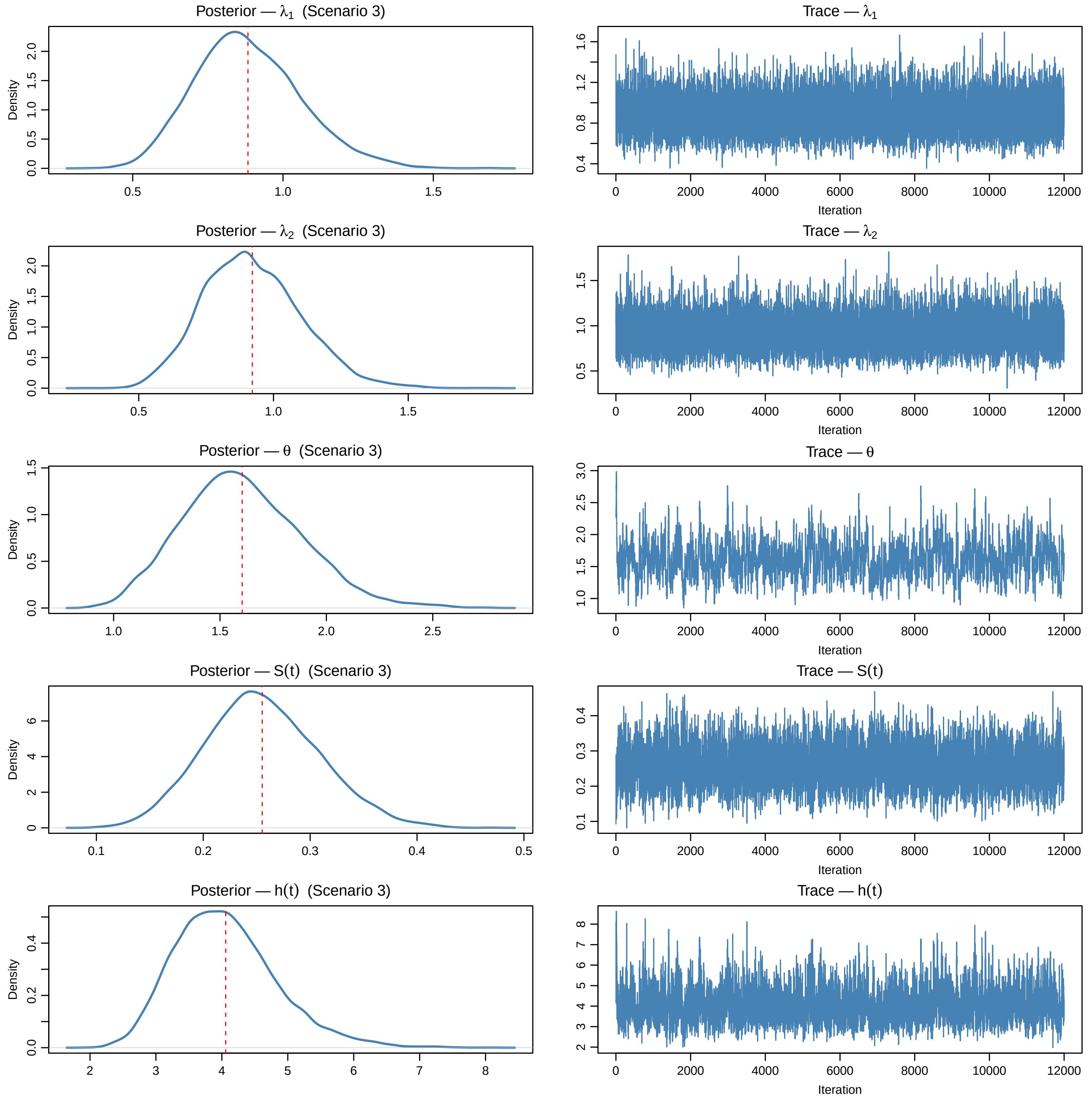

Figure 8. Posterior density plots (left column) and trace plots (right column) for θ, λ_1, λ_2, $S(t_0)$, and $h(t_0)$ under Scenario 3 (M = 12,000, burn-in = 2,000, Prior II). The red dashed line marks the posterior mean.

7.6. Model comparison under IAT-II PCS

Table 12 provides a direct comparison between the Gompertz and Weibull competing risks models fitted to each of the three IAT-II PCS scenarios via the profiles' MLEs. The comparison uses the log-likelihood, AIC, and BIC computed from the IAT-II PCS likelihood of Section 3.

Table 12. Model comparison between the Gompertz and Weibull competing risks models under the three IAT-II PCS electrode scenarios (k = 3 parameters for both models). A lower AIC and BIC indicate better fit. ΔAIC = $\text{AIC}_{\text{Weibull}} - \text{AIC}_{\text{Gompertz}}$.

Scenario	Model	Shape	$\hat{\lambda}_1/\hat{\beta}_1$	$\hat{\lambda}_2/\hat{\beta}_2$	$\log L$	AIC	BIC	ΔAIC
Scenario 1	Gompertz	5.4921	1.0065	0.7908	−5.1322	16.2644	19.9210	6.289
	Weibull	1.0480	2.3357	1.8352	−8.2762	22.5525	26.2091	
Scenario 2	Gompertz	4.5790	1.1052	0.7368	−7.6062	21.2125	24.8691	4.417
	Weibull	0.9968	2.1487	1.4325	−9.8146	25.6291	29.2858	
Scenario 3	Gompertz	2.3581	1.6514	0.6606	−9.2804	24.5607	27.6943	0.517
	Weibull	0.9012	1.9093	0.7637	−9.5388	25.0777	28.2113	

The results in Table 12 show that, within the joint IAT-II PCS competing risks likelihood, the Gompertz model yields lower AIC and BIC values than the Weibull model across all three censored scenarios. For Scenario 1, the Gompertz model achieves AIC = 16.264 compared with 22.553 for the Weibull model, corresponding to ΔAIC = 6.289. For Scenario 2, ΔAIC = 4.417. For Scenario 3, the advantage narrows to ΔAIC = 0.517, reflecting the smaller effective sample size in Case III. The BIC differences follow the same pattern. These results indicate that the Gompertz distribution provides a consistently favorable description of the joint failure process, with a substantial advantage for Scenarios 1 and 2 (ΔAIC > 4) and a marginal advantage for Scenario 3 (ΔAIC = 0.517).

These findings contrast with the marginal goodness-of-fit results in Section 7.2, where the Weibull model fitted Cause 2 better. The explanation is that the IAT-II PCS log-likelihood depends on the joint competing risks structure, including both failure modes, the censoring mechanism, and the interplay between causes. Consequently, the Gompertz model's stronger characterization of the early Cause 1 failures appears to compensate for its weaker marginal fit to the distribution of Cause 2, resulting in a superior joint likelihood for Scenarios 1 and 2 and a comparable fit for Scenario 3.

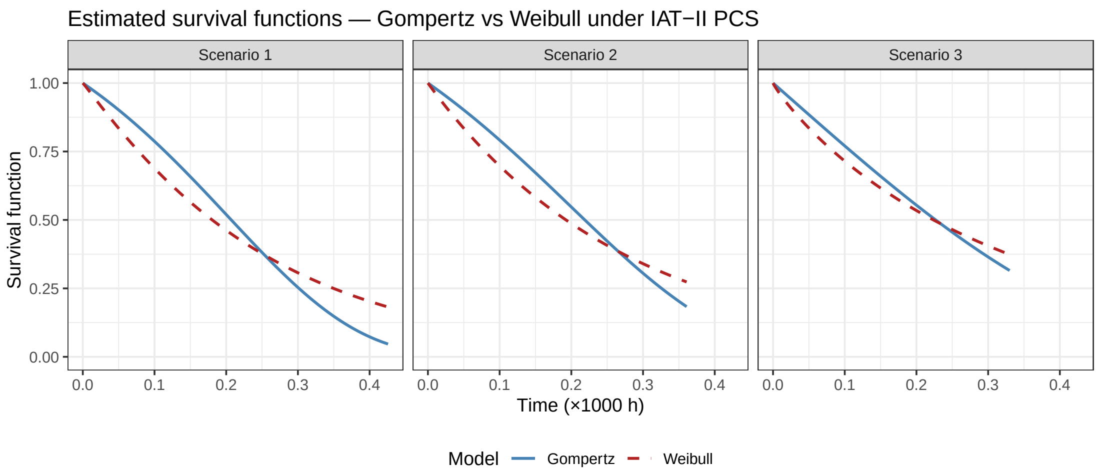

Figure 9. Estimated survival functions under the Gompertz (solid) and Weibull (dashed) competing risks models for the three IAT-II PCS electrode scenarios, obtained from the profile MLEs in Table 12.

Figure 9 presents the estimated survival functions under both models for all three scenarios. In each panel, the Gompertz survival function decreases more steeply at early times, consistent with the exponentially increasing hazard, while the Weibull function declines more gradually. The differences are most pronounced for Scenario 3, reflecting the larger proportion of early Cause 1 failures in that scenario.

8. Conclusions

This paper developed a unified classical and Bayesian inferential framework for competing risks data arising from the Gompertz distribution under the improved adaptive Type II progressive censoring scheme (IAT-II PCS). Operating within the latent failure time formulation of Cox [7], with two stochastically independent competing causes and a shared shape parameter, the proposed framework exploits a distinctive analytical property of the Gompertz log-likelihood: The cause-specific scale parameters λ_1 and λ_2 enter the likelihood in a log-linear fashion, yielding closed-form MLEs as explicit functions of θ and reducing the full three-dimensional optimization to a one-dimensional profile search. This structural feature is absent from the existing Weibull and Nadarajah–Haghighi competing risks formulations studied under IAT-II PCS, where numerical optimization must be performed jointly over all model parameters. Consequently, the proposed Gompertz competing risks model combines analytical tractability with computational efficiency, making it particularly attractive for censored reliability experiments.

In the Bayesian framework, the same log-linear structure produces exact Gamma full conditional posteriors for λ_1 and λ_2, enabling direct Gibbs sampling without rejection for these parameters. Only the shape parameter θ requires an MH update with a log-scale proposal. The resulting hybrid Gibbs–MH sampler achieves effective sample size ratios of 4.6–7.6 for the scale parameters relative to θ across all 32 simulated scenarios, confirming substantially improved mixing and sampling efficiency for λ_1 and λ_2, and improved computational efficiency resulting from direct Gibbs updates for the scale parameters. HPDs' credible intervals are constructed via the Chen–Shao method and are shown to be generally shorter while maintaining coverage probabilities close to the nominal level.

The Monte Carlo simulation study, conducted over a full factorial design of sample sizes, effective failure counts, censoring schemes, and threshold settings, yielded five consistent patterns. First, under moderately informative priors, Bayesian estimators generally outperform the MLE in their finite-sample RMSE and MRAB for all parameters, with the advantage being most pronounced for θ under small samples and heavy right-censoring. Second, the closed-form MLEs of λ_1 and λ_2 exhibit small bias even in moderate samples, confirming the analytical tractability of the scale parameter estimation. Third, the MLE of θ exhibits boundary behavior under heavy censoring and right-heavy schemes, rendering asymptotic confidence intervals based on the Delta method unreliable; the Bayesian framework is therefore the recommended approach whenever inference on θ or the HRF is required. Fourth, balanced and left-heavy censoring schemes consistently outperform right-heavy schemes in estimation accuracy, providing a practical design guideline for experimenters planning life tests under IAT-II PCS. Fifth, HPDs' credible intervals under moderately informative priors achieve the best combination of interval length and nominal coverage across all parameters and reliability characteristics.

Application to the electrode voltage–endurance dataset of Doganaksoy et al. [29] demonstrated the practical utility of the framework across all three censoring cases of the IAT-II PCS. Within the joint competing risks' likelihood, the Gompertz model yielded lower joint AIC and BIC values than the Weibull model for the three IAT-II PCS scenarios considered, with ΔAIC values of 6.3, 4.4, and 0.5 for Scenarios 1, 2, and 3, respectively. Marginal goodness-of-fit analysis revealed, however, that the Weibull distribution provides a superior fit to the surface discharge failure mode (Cause 2, Mode D), where the estimated Gompertz shape parameter implies a physically implausible explosive hazard rate. Although the Weibull distribution provides a superior marginal fit for Cause 2, the Gompertz competing risks model yielded a higher joint likelihood and lower information criteria under the IAT-II PCS framework, suggesting that the Gompertz hazard structure captures the overall competing risks mechanism more effectively when censoring and the causes' interactions are jointly modeled. This asymmetry between the marginal and joint model comparison criteria is itself a finding of practical interest: When failure modes exhibit fundamentally different degradation dynamics, a single parametric family may achieve superior joint likelihood performance while fitting individual causes unevenly.

Limitations

Several limitations of the present study should be acknowledged. The competing risks model assumes the stochastic independence of the latent failure times and a common shape parameter θ across all causes. The independence assumption is standard in the latent failure time literature but is not empirically testable from cause-specific data alone [31], and violations of this assumption may lead to biased cause-specific inference; a detailed discussion of the practical settings in which independence may fail, and of the identifiability consequences, is provided in Remark 3. The common shape constraint, while analytically essential for the closed-form results derived here, restricts the model to failure mechanisms that share the same rate of hazard acceleration, which may not hold in applications where the competing causes represent physically distinct degradation processes operating on different timescales; the rationale for this assumption, and the settings in which it is expected to be adequate, are discussed in Remark 4. The analysis is also restricted to two competing causes, which is adequate for the electrode application considered here; the extension to three or more competing causes is left for future work. Furthermore, the Bayesian results under moderately informative priors are sensitive to the choice of hyperparameters; the prior may exert a substantial influence on posterior inference for θ in small samples, and a formal sensitivity analysis of this issue is reported in Section 6.7: When the prior mean is misspecified by $+100\%$ or -50%, the posterior estimates of θ, $S(t_0)$, and $h(t_0)$ become biased and their credible intervals undercover, whereas a correctly scaled but diffuse prior retains near-nominal performance. Accordingly, an informative prior should be adopted only when supported by genuine external information; otherwise, the weakly informative Prior I or a diffuse, correctly scaled prior is recommended.

Future research

The framework established in this paper opens several directions for future investigation. From a modeling perspective, the most immediate extension is to relax the common shape assumption by allowing cause-specific shape parameters θ_1 and θ_2. A second natural extension is to accommodate three or more competing causes within the same IAT-II PCS structure. Third, incorporating dependent latent failure times through copula-based joint models would substantially broaden the applicability of the framework to settings where shared environmental stressors induce positive dependence between failure mechanisms. Fourth, the present results motivate the development of mixed Gompertz–Weibull competing risks models in which different parametric families are assigned to different causes. Fifth, the optimal design of IAT-II PCS experiments for the Gompertz competing risks model, specifically, the choice of the censoring scheme $\mathbf{R}$, the failure count m, and the threshold pair (T_1, T_2) that minimize the expected posterior interval length or maximize the Fisher information represents an important practical problem that the simulation evidence presented here has already begun to illuminate. Finally, extension to step-stress accelerated life testing settings constitutes a promising avenue for applied reliability research.

In summary, the proposed Gompertz competing risks framework under IAT-II PCS combines analytical tractability, computational efficiency, and strong finite-sample performance. The availability of closed-form MLEs for the scale parameters and exact Gibbs updates in the Bayesian framework distinguishes the model from existing competing risks formulations under adaptive progressive censoring, making it a useful and computationally efficient addition to the reliability and survival analysis literature.

Use of Generative-AI tools declaration

The author declares she has not used Artificial Intelligence (AI) tools in the creation of this article.

Acknowledgments

The researcher would like to thank the Deanship of Graduate Studies and Scientific Research at Qassim University (https://www.qu.edu.sa) for financial support (QU-APC-2026).

Conflict of interest

The author declares no conflict of interest.

References

1. M. A. Almuqrin, M. M. Salah, E. A. Ahmed, Statistical inference for competing risks model with adaptive progressively Type II censored Gompertz life data using industrial and medical applications, *Mathematics,* **10** (2022), 4274. https://doi.org/10.3390/math10224274
2. R. Alotaibi, M. Nassar, A. Elshahhat, Reliability analysis of independent Burr-X competing risks model based on improved adaptive progressively Type II censored samples with applications, *AIMS Math.*, **10** (2025), 15302–15332. https://doi.org/10.3934/math.2025687
3. R. Alotaibi, M. Nassar, A. Elshahhat, Reliability analysis for independent Nadarajah–Haghighi competing risks model employing improved adaptive progressively censored data, *AIMS Math.*, **10** (2025), 15131–15164. https://doi.org/10.3934/math.2025679
4. N. Balakrishnan, E. Cramer, *The art of progressive censoring*, New York: Springer, 2014.

5. N. Balakrishnan, R. A. Sandhu, A simple simulational algorithm for generating progressive Type II censored samples, *Am. Stat.*, **49** (1995), 229–230. https://doi.org/10.1080/00031305.1995.10476120

6. M. H. Chen, Q. M. Shao, Monte Carlo estimation of Bayesian credible and HPD intervals, *J. Comput. Graph. Stat.*, **8** (1999), 69–92. https://doi.org/10.1080/10618600.1999.10474802

7. D. R. Cox, The analysis of exponentially distributed life-times with two types of failure, *J. Roy. Stat. Soc. B*, **21** (1959), 411–421. https://doi.org/10.1111/j.2517-6161.1959.tb00349.x

8. E. Cramer, A. B. Schmiedt, Progressively Type II censored competing risks data from Lomax distributions, *Comput. Stat. Data An.*, **55** (2011), 1285–1303. https://doi.org/10.1016/j.csda.2010.09.017

9. M. J. Crowder, *Classical competing risks*, Boca Raton: Chapman and Hall, 2001.

10. A. Dey, S. Dutta, S. Kayal, *Statistical inference of a competing risks model on improved adaptive type-II progressive censored data*, poster presented at the International Workshop on Reliability Theory and Survival Analysis (IWRTSA-2024), Banaras Hindu University, Varanasi, India, 21–23 December 2024. Available from: `http://hdl.handle.net/2080/4881`.

11. A. Dey, S. Dutta, S. Kayal, Statistical inference of a competing risks model based on improved adaptive type-II progressive censored data under Gompertz lifetime distribution, *arXiv Preprint*, 2026. https://doi.org/10.48550/arXiv.2608.01123

12. S. Dutta, S. Kayal, Inference of a competing risks model with partially observed failure causes under improved adaptive type-II progressive censoring, *Proc. I. Mech. Eng. Part*, **237** (2023), 765–780. https://doi.org/10.1177/1748006X221148330

13. M. M. M. El-Din, A. R. Shafay, M. Nagy, Statistical inference under Type II progressively hybrid censored data with Gompertz lifetimes, *Commun. Stat.-Simul. C.*, **46** (2017), 6827–6848. https://doi.org/10.1080/03610918.2016.1222428

14. A. Elshahhat, M. Nassar, Inference of improved adaptive progressively censored competing risks data for Weibull lifetime models, *Stat. Pap.*, **65** (2024), 1163–1196. https://doi.org/10.1007/s00362-023-01417-0

15. A. Gelman, J. B. Carlin, H. S. Stern, D. B. Rubin, *Bayesian data analysis*, 2 Eds., Boca Raton: Chapman and Hall/CRC, 2004.

16. B. Gompertz, On the nature of the function expressive of the law of human mortality, and on a new mode of determining the value of life contingencies, *Phil. Trans. R. Soc.*, **115** (1825), 513–583. https://doi.org/10.1098/rstl.1825.0026

17. A. Henningsen, O. Toomet, maxLik: A package for maximum likelihood estimation in R, *Computation. Stat.*, **26** (2011), 443–458. https://doi.org/10.1007/s00180-010-0217-1

18. L. Jia, Y. Nian, Y. Jia, Prediction and analysis of coronavirus disease 2019, *PLoS ONE*, **15** (2020), e0233336. https://doi.org/10.1371/journal.pone.0233336

19. D. Kundu, A. Joarder, Analysis of Type II progressively hybrid censored data, *Comput. Stat. Data An.*, **50** (2006), 2509–2528. https://doi.org/10.1016/j.csda.2005.05.002

20. J. F. Lawless, *Statistical models and methods for lifetime data*, 2 Eds., Hoboken: Wiley, 2003.

21. Q. Lü, W. Gui, Statistical inference for Gompertz distribution under adaptive type-II progressive hybrid censoring, *J. Appl. Stat.*, **51** (2024), 451–480. https://doi.org/10.1080/02664763.2022.2144487
22. H. K. T. Ng, D. Kundu, P. S. Chan, Statistical analysis of exponential lifetimes under an adaptive Type II progressive censoring scheme, *Nav. Res. Log.*, **56** (2009), 687–698. https://doi.org/10.1002/nav.20371
23. B. Pareek, D. Kundu, S. Kumar, On progressively censored competing risks data for Weibull distributions, *Comput. Stat. Data An.*, **53** (2009), 4083–4094. https://doi.org/10.1016/j.csda.2009.04.010
24. J. Ren, W. Gui, Statistical analysis of adaptive type-II progressively censored competing risks for Weibull models, *Appl. Math. Model.*, **98** (2021), 323–342. https://doi.org/10.1016/j.apm.2021.05.008
25. J. J. E. Rodriguez, C. Dean, C. Canto, COVID-19 prediction using Gompertz model, *SSRN Electron. J.*, 2020. https://doi.org/10.2139/ssrn.3645441
26. M. M. A. Sobhi, A. A. Soliman, Estimation for the exponentiated Weibull model with adaptive Type II progressive censored schemes, *Appl. Math. Model.*, **40** (2016), 1180–1192. https://doi.org/10.1016/j.apm.2015.06.060
27. S. J. Wu, G. H. Shi, Estimations of Gompertz distribution under the Type I progressive hybrid censoring with competing risks, *J. Stat. Comput. Sim.*, **84** (2014), 1033–1052. https://doi.org/10.1080/00949655.2012.742172
28. W. Yan, P. Li, Y. Yu, Statistical inference for the reliability of Burr-XII distribution under improved adaptive Type II progressive censoring, *Appl. Math. Model.*, **95** (2021), 38–52. https://doi.org/10.1016/j.apm.2021.01.050
29. N. Doganaksoy, G. J. Hahn, W. Q. Meeker, Reliability analysis by failure mode, *Qual. Prog.*, **35** (2002), 47–52.
30. H. W. Lilliefors, On the Kolmogorov–Smirnov test for normality with mean and variance unknown, *J. Am. Stat. Assoc.*, **62** (1967), 399–402. https://doi.org/10.1080/01621459.1967.10482916
31. A. Tsiatis, A nonidentifiability aspect of the problem of competing risks, *P. Natl. Acad. Sci. USA*, **72** (1975), 20–22. https://doi.org/10.1073/pnas.72.1.20
32. Q. Lv, R. Hua, W. Gui, Statistical inference of Gompertz distribution under general progressive type II censored competing risks sample, *Commun. Stat.-Simul. C.*, **53** (2024), 682–701. https://doi.org/10.1080/03610918.2022.2028834
33. J. Wang, Statistical inference for heterogeneous competing risks model under improved adaptive Type II progressive censoring, *Entropy*, **28** (2026), 609. https://doi.org/10.3390/e28060609
34. S. A. Lone, On estimation of Burr type III model using improved adaptive progressive censoring with application to engineering data, *Qual. Reliab. Eng. Int.*, **42** (2026), 1–10. https://doi.org/10.1002/qre.70072
35. S. A. Lone, H. Panahi, Estimation procedures for partially accelerated life test model based on a unified hybrid censored sample from the Gompertz distribution, *Eksploat. Niezawodn.*, **24** (2022), 427–436. https://doi.org/10.17531/ein.2022.3.4

36. S. Asadi, H. Panahi, C. Swarup, S. A. Lone, Inference on adaptive progressive hybrid censored accelerated life test for Gompertz distribution and its evaluation for virus-containing microdroplets data, *Alex. Eng. J.*, **61** (2022), 10071–10084. https://doi.org/10.1016/j.aej.2022.02.061

Supplementary material

Table S1. Average point estimates (RMSE, MRAB) for θ under all scenarios. True value: $\theta_0 = 1.5$.

(T_1, T_2)	(n, m)	Scheme	MLE	Bayes I	Bayes II
(0.4, 0.8)	(40, 20)	U	2.2540 (1.7302, 0.8556)	1.2826 (1.4420, 0.7496)	1.5112 (0.0672, 0.0363)
		L	1.7373 (1.1194, 0.5965)	1.0272 (1.1420, 0.6641)	1.5078 (0.0854, 0.0460)
		M	1.8259 (1.3120, 0.6625)	1.0691 (1.2575, 0.6944)	1.5044 (0.0784, 0.0426)
		R	2.6385 (2.4630, 1.2393)	1.3981 (1.7760, 0.8922)	1.5070 (0.0466, 0.0251)
	(40, 30)	U	1.6664 (0.9134, 0.4835)	1.0443 (1.0426, 0.6010)	1.5083 (0.0932, 0.0498)
		L	1.6166 (0.9042, 0.4810)	0.9972 (1.0429, 0.6142)	1.5035 (0.0924, 0.0493)
		M	1.6224 (0.9331, 0.5019)	1.0034 (1.0476, 0.6077)	1.5025 (0.0888, 0.0474)
		R	1.9165 (1.2628, 0.6614)	1.1799 (1.1922, 0.6740)	1.5110 (0.0778, 0.0421)
	(80, 40)	U	1.8158 (1.0623, 0.5456)	1.0948 (1.1022, 0.6268)	1.5114 (0.0817, 0.0434)
		L	1.6123 (0.7691, 0.4138)	1.0556 (0.9601, 0.5565)	1.5061 (0.0945, 0.0500)
		M	1.5510 (0.7975, 0.4264)	0.9817 (0.9829, 0.5698)	1.4984 (0.0930, 0.0500)
		R	2.0710 (1.6159, 0.8443)	1.1482 (1.3206, 0.7346)	1.5073 (0.0575, 0.0311)
	(80, 60)	U	1.5659 (0.6265, 0.3339)	1.1361 (0.8411, 0.4668)	1.5038 (0.1026, 0.0544)
		L	1.6020 (0.6318, 0.3336)	1.1727 (0.8282, 0.4570)	1.5077 (0.1005, 0.0527)
		M	1.5524 (0.6631, 0.3484)	1.1067 (0.8663, 0.4833)	1.5019 (0.1028, 0.0538)
		R	1.6911 (0.8109, 0.4257)	1.1195 (0.9561, 0.5484)	1.5106 (0.0856, 0.0460)
(0.8, 1.5)	(40, 20)	U	2.2024 (1.6743, 0.8157)	1.2583 (1.4248, 0.7502)	1.5086 (0.0688, 0.0374)
		L	1.8552 (0.9943, 0.4989)	1.1521 (1.0493, 0.5834)	1.5118 (0.0933, 0.0501)
		M	2.0181 (1.2010, 0.5770)	1.2614 (1.1574, 0.6327)	1.5138 (0.0842, 0.0459)
		R	2.6093 (2.4171, 1.2255)	1.4185 (1.7194, 0.8698)	1.5063 (0.0466, 0.0250)
	(40, 30)	U	1.7554 (0.7715, 0.3946)	1.2439 (0.8958, 0.5002)	1.5136 (0.0984, 0.0529)
		L	1.7923 (0.8071, 0.4117)	1.2649 (0.9289, 0.5227)	1.5143 (0.0993, 0.0535)
		M	1.7653 (0.7933, 0.4031)	1.1876 (0.9194, 0.5143)	1.5105 (0.0984, 0.0527)
		R	1.9353 (1.2634, 0.6427)	1.1635 (1.2161, 0.6822)	1.5125 (0.0759, 0.0407)
	(80, 40)	U	1.9033 (1.0027, 0.5040)	1.2118 (1.0424, 0.5870)	1.5163 (0.0824, 0.0450)
		L	1.6683 (0.6306, 0.3227)	1.2576 (0.7770, 0.4210)	1.5098 (0.1052, 0.0555)
		M	1.6792 (0.6583, 0.3346)	1.2100 (0.8040, 0.4421)	1.5063 (0.1003, 0.0535)
		R	2.0135 (1.6078, 0.8238)	1.1393 (1.3481, 0.7498)	1.5073 (0.0559, 0.0296)
	(80, 60)	U	1.6226 (0.4925, 0.2548)	1.3538 (0.6045, 0.3198)	1.5100 (0.1141, 0.0604)
		L	1.6403 (0.5159, 0.2690)	1.3661 (0.6387, 0.3364)	1.5119 (0.1137, 0.0602)
		M	1.6550 (0.5481, 0.2757)	1.3508 (0.6648, 0.3504)	1.5168 (0.1142, 0.0605)
		R	1.6670 (0.8177, 0.4265)	1.1110 (0.9754, 0.5615)	1.5067 (0.0868, 0.0457)

Table S2. Average point estimates (RMSE, MRAB) for λ_1. True: $\lambda_{10} = 0.5$.

(T_1, T_2)	(n, m)	Scheme	MLE	Bayes I	Bayes II
(0.4, 0.8)	(40, 20)	U	0.4762 (0.2467, 0.3870)	0.5856 (0.2832, 0.4215)	0.5050 (0.0779, 0.1218)
		L	0.5155 (0.2966, 0.4462)	0.6417 (0.3545, 0.5253)	0.5045 (0.0799, 0.1257)
		M	0.4902 (0.2384, 0.3711)	0.5814 (0.2710, 0.4123)	0.4986 (0.0734, 0.1165)
		R	0.4583 (0.2470, 0.3999)	0.5596 (0.2588, 0.3939)	0.5030 (0.0771, 0.1230)
	(40, 30)	U	0.5055 (0.2216, 0.3422)	0.6146 (0.2766, 0.4246)	0.5035 (0.0785, 0.1260)
		L	0.5158 (0.2339, 0.3571)	0.6317 (0.2929, 0.4464)	0.5045 (0.0794, 0.1248)
		M	0.5094 (0.2203, 0.3426)	0.6065 (0.2688, 0.4024)	0.5018 (0.0785, 0.1241)
		R	0.4906 (0.2226, 0.3523)	0.5944 (0.2584, 0.4018)	0.5059 (0.0793, 0.1258)
	(80, 40)	U	0.5011 (0.1765, 0.2808)	0.5889 (0.2143, 0.3361)	0.5088 (0.0781, 0.1244)
		L	0.5031 (0.1934, 0.3034)	0.6081 (0.2522, 0.3892)	0.5022 (0.0757, 0.1216)
		M	0.5053 (0.1750, 0.2720)	0.5766 (0.2047, 0.3103)	0.4989 (0.0762, 0.1217)
		R	0.4715 (0.1765, 0.2852)	0.5504 (0.1837, 0.2876)	0.5002 (0.0774, 0.1224)
	(80, 60)	U	0.5008 (0.1548, 0.2447)	0.5785 (0.2048, 0.3082)	0.5005 (0.0743, 0.1181)
		L	0.4957 (0.1560, 0.2484)	0.5777 (0.2038, 0.3138)	0.5003 (0.0730, 0.1160)
		M	0.5095 (0.1522, 0.2351)	0.5808 (0.1908, 0.2947)	0.5045 (0.0736, 0.1158)
		R	0.4889 (0.1482, 0.2379)	0.5730 (0.1876, 0.2917)	0.5007 (0.0731, 0.1148)
(0.8, 1.5)	(40, 20)	U	0.4834 (0.2498, 0.3829)	0.5928 (0.2904, 0.4341)	0.5057 (0.0789, 0.1239)
		L	0.5049 (0.2642, 0.4024)	0.6547 (0.3575, 0.5285)	0.5084 (0.0784, 0.1246)
		M	0.4786 (0.2295, 0.3641)	0.5855 (0.2836, 0.4314)	0.5020 (0.0762, 0.1213)
		R	0.4564 (0.2488, 0.4007)	0.5549 (0.2599, 0.3943)	0.5026 (0.0791, 0.1257)
	(40, 30)	U	0.4941 (0.2130, 0.3328)	0.6017 (0.2837, 0.4279)	0.5038 (0.0788, 0.1242)
		L	0.4889 (0.2061, 0.3278)	0.6074 (0.2833, 0.4351)	0.5063 (0.0752, 0.1208)
		M	0.4969 (0.2076, 0.3231)	0.6039 (0.2733, 0.4144)	0.5052 (0.0809, 0.1278)
		R	0.4853 (0.2144, 0.3429)	0.5944 (0.2537, 0.3989)	0.5049 (0.0789, 0.1261)
	(80, 40)	U	0.4789 (0.1680, 0.2635)	0.5636 (0.2009, 0.3133)	0.5029 (0.0781, 0.1236)
		L	0.4979 (0.1794, 0.2820)	0.5901 (0.2414, 0.3637)	0.5054 (0.0772, 0.1223)
		M	0.5017 (0.1732, 0.2608)	0.5732 (0.2137, 0.3154)	0.5052 (0.0784, 0.1232)
		R	0.4798 (0.1824, 0.2962)	0.5540 (0.1884, 0.2957)	0.5011 (0.0770, 0.1215)
	(80, 60)	U	0.4919 (0.1373, 0.2193)	0.5494 (0.1758, 0.2671)	0.5014 (0.0729, 0.1157)
		L	0.4924 (0.1491, 0.2378)	0.5556 (0.1929, 0.2928)	0.5032 (0.0746, 0.1190)
		M	0.4986 (0.1451, 0.2271)	0.5570 (0.1860, 0.2806)	0.5065 (0.0751, 0.1196)
		R	0.4875 (0.1524, 0.2440)	0.5690 (0.1877, 0.2958)	0.4973 (0.0730, 0.1153)

Table S3. Average point estimates (RMSE, MRAB) for λ_2. True: $\lambda_{20} = 1.0$.

(T_1, T_2)	(n, m)	Scheme	MLE	Bayes I	Bayes II
(0.4, 0.8)	(40, 20)	U	0.9498 (0.3960, 0.3193)	1.1672 (0.4400, 0.3399)	1.0094 (0.1072, 0.0864)
		L	1.0212 (0.4508, 0.3508)	1.2754 (0.5561, 0.4298)	1.0073 (0.1069, 0.0846)
		M	0.9897 (0.3920, 0.3098)	1.1740 (0.4447, 0.3441)	0.9999 (0.1090, 0.0880)
		R	0.9100 (0.4019, 0.3299)	1.1129 (0.3871, 0.3003)	1.0053 (0.1082, 0.0862)
	(40, 30)	U	1.0100 (0.3754, 0.2960)	1.2287 (0.4813, 0.3749)	1.0050 (0.1110, 0.0881)
		L	1.0206 (0.3779, 0.2938)	1.2504 (0.4815, 0.3773)	1.0049 (0.1083, 0.0861)
		M	1.0154 (0.3416, 0.2730)	1.2095 (0.4250, 0.3345)	1.0043 (0.1059, 0.0852)
		R	0.9725 (0.3586, 0.2891)	1.1825 (0.4239, 0.3342)	1.0095 (0.1106, 0.0881)
	(80, 40)	U	0.9959 (0.2959, 0.2351)	1.1688 (0.3576, 0.2837)	1.0139 (0.1089, 0.0854)
		L	1.0062 (0.3271, 0.2519)	1.2129 (0.4245, 0.3364)	1.0042 (0.1050, 0.0827)
		M	1.0228 (0.2801, 0.2178)	1.1681 (0.3442, 0.2738)	1.0047 (0.1047, 0.0835)
		R	0.9556 (0.2999, 0.2441)	1.1158 (0.3084, 0.2434)	1.0069 (0.1120, 0.0891)
	(80, 60)	U	1.0044 (0.2616, 0.2048)	1.1581 (0.3526, 0.2786)	1.0017 (0.1029, 0.0810)
		L	0.9941 (0.2636, 0.2102)	1.1587 (0.3606, 0.2852)	1.0026 (0.1000, 0.0803)
		M	1.0124 (0.2584, 0.2028)	1.1546 (0.3346, 0.2643)	1.0041 (0.1027, 0.0808)
		R	0.9919 (0.2609, 0.2084)	1.1620 (0.3393, 0.2769)	1.0094 (0.1003, 0.0803)
(0.8, 1.5)	(40, 20)	U	0.9482 (0.4050, 0.3212)	1.1642 (0.4480, 0.3471)	1.0044 (0.1066, 0.0850)
		L	0.9807 (0.4160, 0.3245)	1.2708 (0.5548, 0.4345)	1.0069 (0.1031, 0.0812)
		M	0.9772 (0.3914, 0.3100)	1.1939 (0.4849, 0.3789)	1.0090 (0.1091, 0.0866)
		R	0.9104 (0.4165, 0.3333)	1.1029 (0.3937, 0.2982)	1.0024 (0.1072, 0.0859)
	(40, 30)	U	0.9802 (0.3465, 0.2710)	1.1926 (0.4659, 0.3633)	1.0060 (0.1037, 0.0824)
		L	0.9542 (0.3382, 0.2724)	1.1846 (0.4694, 0.3693)	1.0006 (0.1012, 0.0804)
		M	0.9833 (0.3192, 0.2519)	1.1948 (0.4352, 0.3375)	1.0084 (0.1052, 0.0837)
		R	0.9749 (0.3678, 0.2961)	1.1945 (0.4342, 0.3469)	1.0117 (0.1096, 0.0875)
	(80, 40)	U	0.9600 (0.2764, 0.2210)	1.1307 (0.3405, 0.2690)	1.0071 (0.1087, 0.0864)
		L	0.9892 (0.2973, 0.2383)	1.1727 (0.4170, 0.3205)	1.0062 (0.1025, 0.0817)
		M	0.9951 (0.2801, 0.2179)	1.1375 (0.3589, 0.2737)	1.0041 (0.1097, 0.0867)
		R	0.9731 (0.3022, 0.2453)	1.1267 (0.3156, 0.2505)	1.0123 (0.1124, 0.0899)
	(80, 60)	U	0.9912 (0.2372, 0.1869)	1.1062 (0.3136, 0.2390)	1.0063 (0.1026, 0.0801)
		L	0.9763 (0.2420, 0.1938)	1.1018 (0.3288, 0.2522)	1.0013 (0.1005, 0.0796)
		M	0.9880 (0.2329, 0.1853)	1.1021 (0.3059, 0.2347)	1.0072 (0.1030, 0.0826)
		R	0.9981 (0.2666, 0.2134)	1.1648 (0.3462, 0.2818)	1.0100 (0.1037, 0.0830)

Table S4. Average point estimates (RMSE, MRAB) for $S(t_0)$. True: $S_0 = 0.3273$.

(T_1, T_2)	(n, m)	Scheme	MLE	Bayes I	Bayes II
(0.4, 0.8)	(40, 20)	U	0.2923 (0.1054, 0.2521)	0.3268 (0.0848, 0.2036)	0.3281 (0.0349, 0.0861)
		L	0.3231 (0.0930, 0.2263)	0.3283 (0.0845, 0.2055)	0.3293 (0.0364, 0.0895)
		M	0.3190 (0.0952, 0.2313)	0.3443 (0.0886, 0.2165)	0.3327 (0.0363, 0.0893)
		R	0.2747 (0.1350, 0.3175)	0.3337 (0.0997, 0.2442)	0.3300 (0.0348, 0.0856)
	(40, 30)	U	0.3255 (0.0750, 0.1847)	0.3295 (0.0696, 0.1708)	0.3295 (0.0372, 0.0914)
		L	0.3264 (0.0743, 0.1783)	0.3268 (0.0684, 0.1630)	0.3297 (0.0363, 0.0877)
		M	0.3246 (0.0707, 0.1740)	0.3338 (0.0656, 0.1612)	0.3305 (0.0358, 0.0885)
		R	0.3125 (0.0764, 0.1832)	0.3268 (0.0643, 0.1546)	0.3274 (0.0359, 0.0878)
	(80, 40)	U	0.3070 (0.0704, 0.1674)	0.3285 (0.0607, 0.1453)	0.3251 (0.0357, 0.0880)
		L	0.3277 (0.0615, 0.1500)	0.3273 (0.0576, 0.1407)	0.3296 (0.0343, 0.0839)
		M	0.3252 (0.0624, 0.1518)	0.3410 (0.0610, 0.1495)	0.3311 (0.0356, 0.0873)
		R	0.2984 (0.0953, 0.2230)	0.3405 (0.0759, 0.1836)	0.3292 (0.0351, 0.0854)
	(80, 60)	U	0.3288 (0.0520, 0.1266)	0.3299 (0.0498, 0.1208)	0.3303 (0.0342, 0.0836)
		L	0.3294 (0.0513, 0.1257)	0.3279 (0.0489, 0.1192)	0.3297 (0.0327, 0.0803)
		M	0.3254 (0.0504, 0.1237)	0.3302 (0.0479, 0.1178)	0.3289 (0.0336, 0.0827)
		R	0.3213 (0.0496, 0.1192)	0.3293 (0.0439, 0.1054)	0.3274 (0.0322, 0.0788)
(0.8, 1.5)	(40, 20)	U	0.2975 (0.1036, 0.2425)	0.3295 (0.0838, 0.1992)	0.3295 (0.0354, 0.0854)
		L	0.3208 (0.0910, 0.2179)	0.3174 (0.0812, 0.1933)	0.3279 (0.0353, 0.0852)
		M	0.3067 (0.0943, 0.2292)	0.3256 (0.0802, 0.1933)	0.3287 (0.0353, 0.0869)
		R	0.2766 (0.1302, 0.3103)	0.3348 (0.0961, 0.2361)	0.3309 (0.0339, 0.0823)
	(40, 30)	U	0.3257 (0.0732, 0.1776)	0.3234 (0.0682, 0.1650)	0.3285 (0.0343, 0.0831)
		L	0.3300 (0.0738, 0.1807)	0.3243 (0.0697, 0.1707)	0.3290 (0.0335, 0.0822)
		M	0.3202 (0.0725, 0.1771)	0.3229 (0.0655, 0.1596)	0.3279 (0.0355, 0.0877)
		R	0.3122 (0.0778, 0.1903)	0.3264 (0.0651, 0.1609)	0.3270 (0.0362, 0.0906)
	(80, 40)	U	0.3112 (0.0684, 0.1633)	0.3306 (0.0594, 0.1438)	0.3276 (0.0350, 0.0859)
		L	0.3260 (0.0612, 0.1506)	0.3213 (0.0588, 0.1454)	0.3279 (0.0329, 0.0799)
		M	0.3201 (0.0617, 0.1479)	0.3289 (0.0562, 0.1349)	0.3289 (0.0350, 0.0853)
		R	0.2985 (0.0929, 0.2119)	0.3385 (0.0751, 0.1811)	0.3277 (0.0344, 0.0853)
	(80, 60)	U	0.3271 (0.0527, 0.1280)	0.3251 (0.0514, 0.1257)	0.3284 (0.0335, 0.0811)
		L	0.3296 (0.0518, 0.1255)	0.3257 (0.0515, 0.1256)	0.3289 (0.0314, 0.0764)
		M	0.3227 (0.0507, 0.1242)	0.3235 (0.0483, 0.1186)	0.3262 (0.0329, 0.0806)
		R	0.3230 (0.0502, 0.1210)	0.3307 (0.0452, 0.1088)	0.3285 (0.0330, 0.0808)

Table S5. Average point estimates (RMSE, MRAB) for $h(t_0)$. True: $h_0 = 3.1755$.

(T_1, T_2)	(n, m)	Scheme	MLE	Bayes I	Bayes II
(0.4, 0.8)	(40, 20)	U	5.2398 (12.8512, 0.7963)	4.3582 (15.4707, 0.6703)	3.2499 (0.3586, 0.0913)
		L	3.5938 (1.6294, 0.3080)	3.1217 (1.3605, 0.2734)	3.2376 (0.3864, 0.0958)
		M	4.0536 (6.9393, 0.4833)	3.4074 (7.5063, 0.4342)	3.2051 (0.3618, 0.0921)
		R	7.3868 (15.5701, 1.5268)	6.5417 (23.5824, 1.4127)	3.2311 (0.3396, 0.0869)
	(40, 30)	U	3.4262 (1.0987, 0.2351)	3.0208 (0.9827, 0.2240)	3.2277 (0.3894, 0.0973)
		L	3.3617 (0.9523, 0.2156)	2.9912 (0.8614, 0.2125)	3.2205 (0.3774, 0.0930)
		M	3.4102 (1.1090, 0.2440)	2.9742 (0.9959, 0.2357)	3.2135 (0.3687, 0.0927)
		R	3.8598 (1.8722, 0.3615)	3.2641 (1.4875, 0.3027)	3.2477 (0.3734, 0.0935)
	(80, 40)	U	3.8131 (1.7896, 0.3302)	3.1930 (1.5632, 0.2976)	3.2633 (0.3748, 0.0937)
		L	3.3152 (0.7691, 0.1788)	2.9887 (0.7534, 0.1882)	3.2144 (0.3557, 0.0888)
		M	3.3429 (1.0105, 0.2274)	2.8995 (0.9735, 0.2425)	3.2002 (0.3622, 0.0902)
		R	4.6056 (4.0964, 0.6562)	3.6758 (3.7097, 0.5198)	3.2257 (0.3477, 0.0863)
	(80, 60)	U	3.2526 (0.6038, 0.1472)	2.9904 (0.6351, 0.1644)	3.1980 (0.3465, 0.0868)
		L	3.2672 (0.5802, 0.1401)	3.0224 (0.5992, 0.1524)	3.2045 (0.3350, 0.0839)
		M	3.2841 (0.6989, 0.1617)	2.9883 (0.7289, 0.1820)	3.2103 (0.3477, 0.0861)
		R	3.4443 (0.9130, 0.2035)	3.0346 (0.8507, 0.2098)	3.2279 (0.3331, 0.0827)
(0.8, 1.5)	(40, 20)	U	4.9135 (6.7548, 0.6960)	3.9987 (6.7199, 0.5632)	3.2363 (0.3605, 0.0899)
		L	3.6657 (1.5361, 0.2759)	3.2447 (1.2946, 0.2272)	3.2482 (0.3811, 0.0942)
		M	4.0734 (2.3080, 0.3987)	3.4113 (1.8682, 0.3240)	3.2445 (0.3663, 0.0933)
		R	7.0972 (15.1062, 1.4432)	7.3592 (40.2488, 1.6604)	3.2225 (0.3319, 0.0824)
	(40, 30)	U	3.4494 (0.8810, 0.1915)	3.1504 (0.7364, 0.1722)	3.2335 (0.3645, 0.0902)
		L	3.4375 (0.9408, 0.1887)	3.1559 (0.8168, 0.1697)	3.2276 (0.3578, 0.0887)
		M	3.5370 (1.0687, 0.2222)	3.1517 (0.8826, 0.2001)	3.2396 (0.3797, 0.0948)
		R	3.8712 (1.8569, 0.3555)	3.2553 (1.5211, 0.3011)	3.2525 (0.3777, 0.0959)
	(80, 40)	U	3.8122 (1.6421, 0.3138)	3.2290 (1.4137, 0.2846)	3.2432 (0.3647, 0.0909)
		L	3.3555 (0.6709, 0.1519)	3.1413 (0.5956, 0.1420)	3.2270 (0.3508, 0.0863)
		M	3.4509 (0.9224, 0.1888)	3.1001 (0.8235, 0.1849)	3.2211 (0.3620, 0.0896)
		R	4.5629 (4.3603, 0.6391)	3.7245 (4.4181, 0.5397)	3.2389 (0.3449, 0.0867)
	(80, 60)	U	3.3030 (0.5704, 0.1304)	3.1568 (0.5280, 0.1269)	3.2162 (0.3548, 0.0865)
		L	3.2862 (0.5305, 0.1208)	3.1513 (0.5004, 0.1175)	3.2102 (0.3312, 0.0809)
		M	3.3679 (0.6217, 0.1421)	3.1771 (0.5746, 0.1363)	3.2407 (0.3481, 0.0870)
		R	3.4113 (0.9108, 0.2003)	3.0189 (0.8751, 0.2165)	3.2158 (0.3358, 0.0839)

Table S6. Average point estimates (RMSE, MRAB) for π_1. True: $\pi_{10} = 0.3333$.

(T_1, T_2)	(n, m)	Scheme	MLE	Bayes I	Bayes II
(0.4, 0.8)	(40, 20)	U	0.3336 (0.1068, 0.2547)	0.3336 (0.1067, 0.2545)	0.3334 (0.0427, 0.1019)
		L	0.3341 (0.1157, 0.2760)	0.3342 (0.1158, 0.2761)	0.3336 (0.0436, 0.1040)
		M	0.3326 (0.1102, 0.2607)	0.3326 (0.1102, 0.2608)	0.3330 (0.0421, 0.0999)
		R	0.3338 (0.1047, 0.2523)	0.3338 (0.1048, 0.2524)	0.3335 (0.0419, 0.1010)
	(40, 30)	U	0.3344 (0.0918, 0.2191)	0.3345 (0.0918, 0.2192)	0.3339 (0.0437, 0.1043)
		L	0.3353 (0.0936, 0.2241)	0.3353 (0.0935, 0.2241)	0.3343 (0.0443, 0.1063)
		M	0.3330 (0.0902, 0.2159)	0.3330 (0.0902, 0.2159)	0.3331 (0.0433, 0.1035)
		R	0.3344 (0.0881, 0.2104)	0.3344 (0.0880, 0.2106)	0.3339 (0.0440, 0.1054)
	(80, 40)	U	0.3346 (0.0724, 0.1729)	0.3346 (0.0724, 0.1730)	0.3341 (0.0414, 0.0988)
		L	0.3337 (0.0789, 0.1890)	0.3337 (0.0789, 0.1893)	0.3335 (0.0431, 0.1032)
		M	0.3304 (0.0744, 0.1799)	0.3304 (0.0744, 0.1801)	0.3317 (0.0411, 0.0995)
		R	0.3310 (0.0754, 0.1800)	0.3310 (0.0754, 0.1800)	0.3320 (0.0431, 0.1028)
	(80, 60)	U	0.3331 (0.0635, 0.1512)	0.3331 (0.0635, 0.1512)	0.3332 (0.0409, 0.0974)
		L	0.3327 (0.0636, 0.1523)	0.3327 (0.0636, 0.1523)	0.3329 (0.0409, 0.0980)
		M	0.3351 (0.0621, 0.1467)	0.3351 (0.0621, 0.1468)	0.3344 (0.0402, 0.0951)
		R	0.3306 (0.0605, 0.1427)	0.3306 (0.0605, 0.1429)	0.3315 (0.0404, 0.0953)
(0.8, 1.5)	(40, 20)	U	0.3375 (0.1057, 0.2563)	0.3372 (0.1062, 0.2571)	0.3348 (0.0425, 0.1028)
		L	0.3385 (0.1070, 0.2588)	0.3385 (0.1070, 0.2587)	0.3354 (0.0428, 0.1034)
		M	0.3308 (0.1075, 0.2620)	0.3309 (0.1075, 0.2620)	0.3324 (0.0430, 0.1048)
		R	0.3347 (0.1086, 0.2622)	0.3348 (0.1086, 0.2621)	0.3339 (0.0435, 0.1050)
	(40, 30)	U	0.3338 (0.0867, 0.2019)	0.3338 (0.0867, 0.2020)	0.3335 (0.0433, 0.1012)
		L	0.3386 (0.0842, 0.1999)	0.3386 (0.0842, 0.2002)	0.3360 (0.0421, 0.1002)
		M	0.3339 (0.0874, 0.2058)	0.3338 (0.0874, 0.2061)	0.3336 (0.0437, 0.1031)
		R	0.3324 (0.0848, 0.2003)	0.3325 (0.0848, 0.2007)	0.3329 (0.0425, 0.1005)
	(80, 40)	U	0.3329 (0.0758, 0.1811)	0.3329 (0.0758, 0.1812)	0.3331 (0.0433, 0.1035)
		L	0.3351 (0.0760, 0.1824)	0.3351 (0.0760, 0.1824)	0.3343 (0.0434, 0.1042)
		M	0.3359 (0.0747, 0.1792)	0.3359 (0.0747, 0.1793)	0.3348 (0.0427, 0.1025)
		R	0.3297 (0.0756, 0.1806)	0.3297 (0.0756, 0.1805)	0.3313 (0.0432, 0.1031)
	(80, 60)	U	0.3322 (0.0604, 0.1423)	0.3322 (0.0604, 0.1425)	0.3326 (0.0402, 0.0949)
		L	0.3350 (0.0631, 0.1518)	0.3350 (0.0631, 0.1519)	0.3345 (0.0421, 0.1013)
		M	0.3352 (0.0613, 0.1459)	0.3352 (0.0614, 0.1461)	0.3346 (0.0409, 0.0973)
		R	0.3284 (0.0618, 0.1471)	0.3284 (0.0618, 0.1473)	0.3300 (0.0412, 0.0982)

Table S7. Average confidence/credible length and coverage probability (ACL, CP) for θ. Nominal level: 95%.

(T_1, T_2)	(n, m)	Scheme	ACI-MLE	HPD Bayes I	HPD Bayes II
(0.4,0.8)	(40, 20)	U	4.6819 (0.8890)	2.9877 (0.6920)	1.0226 (1.0000)
		L	3.5169 (0.8950)	2.3117 (0.6600)	0.9908 (1.0000)
		M	3.5378 (0.8720)	2.3602 (0.6530)	1.0038 (1.0000)
		R	6.4509 (0.8160)	3.6720 (0.6440)	1.0378 (1.0000)
	(40, 30)	U	3.0256 (0.9280)	2.1375 (0.6790)	0.9681 (1.0000)
		L	3.0126 (0.9180)	2.1171 (0.6880)	0.9627 (1.0000)
		M	3.0331 (0.9270)	2.1165 (0.6740)	0.9736 (1.0000)
		R	3.8461 (0.9110)	2.5934 (0.7030)	0.9997 (1.0000)
	(80, 40)	U	3.3943 (0.9310)	2.3616 (0.7090)	0.9949 (1.0000)
		L	2.7332 (0.9450)	2.0621 (0.7150)	0.9445 (1.0000)
		M	2.6827 (0.9350)	1.9459 (0.6760)	0.9637 (1.0000)
		R	4.7145 (0.8540)	2.9008 (0.6780)	1.0271 (1.0000)
	(80, 60)	U	2.3179 (0.9540)	1.9128 (0.7530)	0.9153 (1.0000)
		L	2.3642 (0.9510)	1.9763 (0.7770)	0.9143 (1.0000)
		M	2.3507 (0.9380)	1.9277 (0.7510)	0.9271 (1.0000)
		R	2.9070 (0.9550)	2.2147 (0.7480)	0.9630 (1.0000)
(0.8,1.5)	(40, 20)	U	4.4844 (0.8969)	2.8864 (0.6950)	1.0151 (1.0000)
		L	3.2186 (0.9370)	2.3967 (0.7440)	0.9621 (0.9990)
		M	3.3938 (0.9150)	2.5358 (0.7300)	0.9880 (1.0000)
		R	6.4065 (0.8140)	3.7703 (0.6840)	1.0378 (1.0000)
	(40, 30)	U	2.6343 (0.9400)	2.1785 (0.7840)	0.9335 (1.0000)
		L	2.6636 (0.9480)	2.1999 (0.7780)	0.9275 (1.0000)
		M	2.7121 (0.9470)	2.1913 (0.7600)	0.9431 (1.0000)
		R	3.8616 (0.8940)	2.5845 (0.6940)	1.0001 (1.0000)
	(80, 40)	U	3.2882 (0.9380)	2.4424 (0.7620)	0.9879 (1.0000)
		L	2.2816 (0.9450)	2.0389 (0.8030)	0.8982 (0.9980)
		M	2.3454 (0.9550)	2.0704 (0.8140)	0.9272 (0.9990)
		R	4.6487 (0.8420)	2.8438 (0.6740)	1.0270 (1.0000)
	(80, 60)	U	1.8588 (0.9520)	1.8287 (0.8740)	0.8587 (0.9980)
		L	1.8717 (0.9430)	1.8244 (0.8500)	0.8555 (1.0000)
		M	1.9246 (0.9340)	1.8746 (0.8510)	0.8792 (1.0000)
		R	2.8772 (0.9390)	2.1593 (0.7390)	0.9600 (1.0000)

Table S8. ACL (CP) for λ_1 and λ_2. Nominal level: 95%.

(T_1, T_2)	(n, m)	Sch	λ_1 ACI	λ_1 HPD-I	λ_1 HPD-II	λ_2 ACI	λ_2 HPD-I	λ_2 HPD-II
(0.4,0.8)	(40, 20)	U	0.9011 (0.857)	0.9245 (0.911)	0.4755 (0.997)	1.5297 (0.892)	1.4717 (0.930)	0.6827 (0.999)
		L	1.0143 (0.877)	1.0658 (0.922)	0.4846 (0.997)	1.7490 (0.898)	1.7047 (0.908)	0.6980 (0.998)
		M	0.9014 (0.894)	0.9279 (0.922)	0.4761 (0.999)	1.4844 (0.893)	1.4692 (0.929)	0.6851 (0.997)
		R	0.8965 (0.848)	0.8812 (0.927)	0.4728 (0.998)	1.5661 (0.869)	1.4023 (0.938)	0.6775 (0.999)
	(40, 30)	U	0.8422 (0.899)	0.8754 (0.913)	0.4469 (0.995)	1.4109 (0.904)	1.4038 (0.894)	0.6465 (0.993)
		L	0.8750 (0.883)	0.9063 (0.917)	0.4487 (0.995)	1.4678 (0.912)	1.4530 (0.892)	0.6487 (0.997)
		M	0.8242 (0.905)	0.8437 (0.918)	0.4443 (0.998)	1.3642 (0.934)	1.3467 (0.922)	0.6418 (0.998)
		R	0.8213 (0.877)	0.8217 (0.916)	0.4387 (0.996)	1.3968 (0.899)	1.3261 (0.888)	0.6325 (0.997)
	(80, 40)	U	0.6837 (0.921)	0.7009 (0.919)	0.4096 (0.991)	1.1336 (0.923)	1.1107 (0.908)	0.5904 (0.993)
		L	0.7469 (0.910)	0.7869 (0.921)	0.4195 (0.996)	1.2627 (0.919)	1.2810 (0.887)	0.6103 (0.998)
		M	0.6705 (0.927)	0.6917 (0.945)	0.4110 (0.992)	1.0922 (0.932)	1.0940 (0.918)	0.5960 (0.998)
		R	0.6887 (0.888)	0.6593 (0.929)	0.4023 (0.991)	1.1858 (0.885)	1.0580 (0.919)	0.5798 (0.991)
	(80, 60)	U	0.5988 (0.929)	0.6334 (0.901)	0.3754 (0.987)	1.0081 (0.926)	1.0392 (0.870)	0.5506 (0.992)
		L	0.6110 (0.918)	0.6503 (0.910)	0.3768 (0.989)	1.0399 (0.924)	1.0812 (0.877)	0.5551 (0.994)
		M	0.5882 (0.939)	0.6202 (0.929)	0.3745 (0.988)	0.9731 (0.928)	1.0012 (0.894)	0.5458 (0.995)
		R	0.5898 (0.918)	0.6106 (0.921)	0.3635 (0.985)	1.0219 (0.924)	1.0132 (0.858)	0.5333 (0.994)
(0.8,1.5)	(40, 20)	U	0.9064 (0.862)	0.9307 (0.915)	0.4753 (0.999)	1.5037 (0.870)	1.4619 (0.918)	0.6808 (0.999)
		L	0.9668 (0.886)	1.0694 (0.908)	0.4804 (1.000)	1.6204 (0.895)	1.7103 (0.923)	0.6907 (1.000)
		M	0.8637 (0.869)	0.9280 (0.912)	0.4745 (0.992)	1.4352 (0.889)	1.4949 (0.913)	0.6848 (0.998)
		R	0.8908 (0.830)	0.8795 (0.927)	0.4719 (0.996)	1.5645 (0.842)	1.3958 (0.934)	0.6760 (0.999)
	(40, 30)	U	0.7796 (0.880)	0.8453 (0.904)	0.4403 (0.992)	1.2974 (0.909)	1.3790 (0.889)	0.6393 (0.997)
		L	0.7862 (0.886)	0.8648 (0.902)	0.4418 (0.997)	1.3029 (0.898)	1.4008 (0.871)	0.6393 (0.999)
		M	0.7647 (0.898)	0.8333 (0.908)	0.4401 (0.994)	1.2573 (0.921)	1.3442 (0.904)	0.6377 (0.994)
		R	0.8152 (0.874)	0.8226 (0.915)	0.4386 (0.995)	1.3976 (0.886)	1.3331 (0.884)	0.6336 (0.997)
	(80, 40)	U	0.6474 (0.898)	0.6790 (0.929)	0.4060 (0.987)	1.0765 (0.912)	1.0895 (0.908)	0.5867 (0.991)
		L	0.6902 (0.913)	0.7567 (0.922)	0.4135 (0.994)	1.1530 (0.924)	1.2494 (0.898)	0.6044 (0.996)
		M	0.6368 (0.933)	0.6840 (0.941)	0.4085 (0.992)	1.0196 (0.924)	1.0874 (0.905)	0.5908 (0.989)
		R	0.6962 (0.888)	0.6603 (0.926)	0.4033 (0.987)	1.2012 (0.892)	1.0617 (0.923)	0.5829 (0.992)
	(80, 60)	U	0.5498 (0.925)	0.5948 (0.927)	0.3688 (0.984)	0.9201 (0.937)	0.9977 (0.913)	0.5471 (0.985)
		L	0.5601 (0.904)	0.6100 (0.906)	0.3708 (0.983)	0.9360 (0.909)	1.0202 (0.908)	0.5487 (0.993)
		M	0.5417 (0.917)	0.5857 (0.914)	0.3694 (0.985)	0.8874 (0.918)	0.9608 (0.914)	0.5424 (0.989)
		R	0.5873 (0.909)	0.6031 (0.914)	0.3619 (0.980)	1.0237 (0.925)	1.0067 (0.854)	0.5331 (0.993)

Table S9. ACL (CP) for $S(t_0)$ and π_1. Nominal level: 95%.

			$S(t_0)$			π_1		
(T_1, T_2)	(n, m)	Sch	ACI-MLE	HPD-I	HPD-II	ACI-MLE	HPD-I	HPD-II
(0.4, 0.8)	(40, 20)	U	0.3338 (0.882)	0.3185 (0.938)	0.2114 (0.998)	0.3999 (0.925)	0.3802 (0.903)	0.2548 (0.995)
		L	0.3460 (0.903)	0.3226 (0.936)	0.2109 (0.996)	0.4182 (0.911)	0.3956 (0.891)	0.2595 (0.995)
		M	0.3373 (0.892)	0.3191 (0.923)	0.2130 (0.996)	0.4129 (0.911)	0.3911 (0.891)	0.2581 (1.000)
		R	0.4015 (0.871)	0.3524 (0.929)	0.2145 (0.994)	0.4005 (0.925)	0.3807 (0.900)	0.2548 (0.999)
	(40, 30)	U	0.2798 (0.921)	0.2670 (0.938)	0.1919 (0.992)	0.3464 (0.925)	0.3333 (0.925)	0.2386 (0.996)
		L	0.2881 (0.924)	0.2701 (0.937)	0.1916 (0.994)	0.3477 (0.920)	0.3347 (0.917)	0.2391 (0.994)
		M	0.2762 (0.932)	0.2644 (0.955)	0.1926 (0.997)	0.3444 (0.925)	0.3315 (0.923)	0.2377 (0.994)
		R	0.2729 (0.918)	0.2577 (0.956)	0.1902 (0.988)	0.3307 (0.947)	0.3193 (0.946)	0.2331 (0.990)
	(80, 40)	U	0.2408 (0.920)	0.2323 (0.942)	0.1774 (0.986)	0.2885 (0.935)	0.2809 (0.935)	0.2166 (0.990)
		L	0.2481 (0.943)	0.2364 (0.961)	0.1771 (0.989)	0.3027 (0.933)	0.2940 (0.936)	0.2225 (0.992)
		M	0.2380 (0.932)	0.2324 (0.949)	0.1796 (0.993)	0.2978 (0.943)	0.2895 (0.943)	0.2205 (0.994)
		R	0.3244 (0.923)	0.2739 (0.914)	0.1822 (0.989)	0.2873 (0.916)	0.2798 (0.916)	0.2161 (0.989)
	(80, 60)	U	0.1967 (0.930)	0.1928 (0.945)	0.1560 (0.975)	0.2480 (0.943)	0.2431 (0.941)	0.1976 (0.978)
		L	0.1992 (0.945)	0.1958 (0.952)	0.1559 (0.983)	0.2484 (0.937)	0.2436 (0.938)	0.1978 (0.985)
		M	0.1922 (0.929)	0.1897 (0.954)	0.1564 (0.983)	0.2465 (0.941)	0.2417 (0.942)	0.1968 (0.981)
		R	0.1874 (0.933)	0.1846 (0.962)	0.1538 (0.982)	0.2358 (0.947)	0.2316 (0.946)	0.1912 (0.983)
(0.8, 1.5)	(40, 20)	U	0.3271 (0.893)	0.3166 (0.952)	0.2109 (0.996)	0.4019 (0.939)	0.3817 (0.909)	0.2551 (0.998)
		L	0.3328 (0.904)	0.3156 (0.932)	0.2048 (0.995)	0.4019 (0.929)	0.3821 (0.906)	0.2552 (0.998)
		M	0.3130 (0.879)	0.3081 (0.933)	0.2084 (0.997)	0.3983 (0.914)	0.3787 (0.902)	0.2543 (0.997)
		R	0.4106 (0.886)	0.3568 (0.930)	0.2146 (0.998)	0.3996 (0.920)	0.3800 (0.895)	0.2548 (0.999)
	(40, 30)	U	0.2719 (0.926)	0.2628 (0.938)	0.1854 (0.995)	0.3309 (0.950)	0.3194 (0.949)	0.2332 (0.989)
		L	0.2786 (0.924)	0.2674 (0.942)	0.1852 (0.997)	0.3325 (0.955)	0.3214 (0.955)	0.2337 (0.993)
		M	0.2637 (0.923)	0.2571 (0.941)	0.1866 (0.992)	0.3308 (0.944)	0.3196 (0.941)	0.2332 (0.992)
		R	0.2712 (0.922)	0.2577 (0.965)	0.1902 (0.996)	0.3307 (0.946)	0.3193 (0.945)	0.2333 (0.992)
	(80, 40)	U	0.2333 (0.931)	0.2306 (0.958)	0.1771 (0.990)	0.2877 (0.914)	0.2802 (0.914)	0.2163 (0.984)
		L	0.2417 (0.939)	0.2339 (0.944)	0.1704 (0.996)	0.2882 (0.924)	0.2807 (0.924)	0.2165 (0.984)
		M	0.2245 (0.916)	0.2226 (0.945)	0.1735 (0.984)	0.2885 (0.936)	0.2811 (0.936)	0.2166 (0.991)
		R	0.3252 (0.925)	0.2718 (0.930)	0.1822 (0.994)	0.2870 (0.921)	0.2797 (0.921)	0.2161 (0.983)
	(80, 60)	U	0.1941 (0.932)	0.1909 (0.940)	0.1498 (0.973)	0.2361 (0.939)	0.2318 (0.938)	0.1913 (0.977)
		L	0.1989 (0.944)	0.1952 (0.937)	0.1496 (0.982)	0.2364 (0.930)	0.2322 (0.930)	0.1916 (0.976)
		M	0.1879 (0.934)	0.1852 (0.947)	0.1505 (0.979)	0.2366 (0.946)	0.2323 (0.946)	0.1917 (0.977)
		R	0.1886 (0.938)	0.1844 (0.960)	0.1537 (0.979)	0.2353 (0.936)	0.2311 (0.934)	0.1910 (0.976)

Table S10. ACL (CP) for $h(t_0)$. Nominal level: 95%.

(T_1, T_2)	(n, m)	Scheme	ACI-MLE	HPD Bayes I	HPD Bayes II
(0.4,0.8)	(40, 20)	U	10.2544 (0.954)	7.9193 (0.839)	2.2607 (0.996)
		L	4.3118 (0.951)	3.4195 (0.867)	2.1923 (0.995)
		M	6.0544 (0.941)	4.7087 (0.809)	2.2178 (0.995)
		R	20.5980 (0.896)	18.4119 (0.750)	2.3011 (0.995)
	(40, 30)	U	3.3518 (0.943)	2.7623 (0.848)	1.9939 (0.991)
		L	3.2032 (0.933)	2.6705 (0.851)	1.9752 (0.990)
		M	3.5659 (0.935)	2.8461 (0.819)	2.0038 (0.993)
		R	5.2230 (0.943)	3.7708 (0.827)	2.0390 (0.988)
	(80, 40)	U	4.7979 (0.958)	3.5418 (0.799)	1.9519 (0.990)
		L	2.7347 (0.952)	2.3692 (0.851)	1.8236 (0.990)
		M	3.3290 (0.936)	2.6683 (0.757)	1.8943 (0.991)
		R	9.4831 (0.900)	6.3802 (0.711)	2.0202 (0.992)
	(80, 60)	U	2.2458 (0.941)	2.0272 (0.830)	1.6097 (0.977)
		L	2.1891 (0.945)	2.0034 (0.866)	1.5992 (0.984)
		M	2.4394 (0.946)	2.1652 (0.826)	1.6468 (0.988)
		R	3.1481 (0.967)	2.5531 (0.805)	1.6749 (0.988)
(0.8,1.5)	(40, 20)	U	9.1540 (0.969)	6.7843 (0.829)	2.2394 (0.993)
		L	3.8351 (0.961)	3.2963 (0.936)	2.1130 (0.990)
		M	5.1867 (0.974)	4.1432 (0.904)	2.1890 (0.994)
		R	19.9992 (0.902)	21.3636 (0.765)	2.2939 (0.998)
	(40, 30)	U	2.8396 (0.967)	2.5746 (0.947)	1.8975 (0.990)
		L	2.7645 (0.963)	2.5318 (0.952)	1.8788 (0.994)
		M	3.1302 (0.963)	2.7761 (0.915)	1.9350 (0.988)
		R	5.2298 (0.964)	3.7449 (0.822)	2.0428 (0.993)
	(80, 40)	U	4.4714 (0.980)	3.4780 (0.817)	1.9247 (0.994)
		L	2.3085 (0.954)	2.1834 (0.940)	1.7182 (0.987)
		M	2.8329 (0.967)	2.5822 (0.889)	1.8140 (0.987)
		R	9.3855 (0.890)	6.4531 (0.708)	2.0288 (0.997)
	(80, 60)	U	1.8727 (0.937)	1.8357 (0.923)	1.5031 (0.968)
		L	1.8150 (0.949)	1.7768 (0.939)	1.4825 (0.984)
		M	2.0329 (0.945)	1.9777 (0.922)	1.5566 (0.984)
		R	3.1011 (0.959)	2.4993 (0.795)	1.6653 (0.983)

To assess the robustness of the proposed procedures under more challenging conditions, we also report an additional small-sample study. The hybrid Gibbs–MH sampler, the profile MLE, and all performance measures are exactly as described in Section 6; only the sample sizes differ. Two very small, heavily censored designs, $(n, m) = (20, 10)$ and $(30, 15)$, are examined under all four censoring schemes with $(T_1, T_2) = (0.4, 0.8)$ and $G = 1{,}000$ replications. Tables S11 and S12 report the point and interval estimation results. The patterns observed for the larger sample sizes in Section 6 persist and become more pronounced. In particular, the MLE and the weakly informative Bayes I estimator of the hazard rate $h(t_0)$ can be extremely unstable in very small and heavily censored samples, especially under the right-heavy censoring scheme, as reflected by the very large RMSE values and interval lengths. By contrast, Bayes II remains substantially more stable across the examined settings. Since Prior II is centered at the data-generating parameter values, these results should be interpreted as a best-case benchmark for situations in which reliable prior information is available. Overall, the small-sample study supports the use of moderately informative Bayesian inference for θ and $h(t_0)$ when the sample is small and censoring is severe, provided that reliable prior information is available.

Table S11. Small-sample study: Average point estimates (RMSE, MRAB) for $(n, m) = (20, 10)$ and $(30, 15)$ under all four censoring schemes, $(T_1, T_2) = (0.4, 0.8)$, $G = 1{,}000$, Prior I, and Prior II. True values: $\theta_0 = 1.5$, $\lambda_{10} = 0.5$, $\lambda_{20} = 1.0$, $S_0(t_0) = 0.3273$, $h_0(t_0) = 3.1755$, and $\pi_{10} = 0.3333$.

(n, m)	Scheme	Param	MLE	Bayes I	Bayes II
(20, 10)	U	θ	3.0595 (2.9712, 1.4195)	1.7269 (2.0886, 1.0000)	1.5056 (0.0513, 0.0273)
		λ_1	0.4571 (0.3376, 0.5291)	0.5816 (0.3770, 0.5613)	0.5022 (0.0659, 0.1060)
		λ_2	0.8907 (0.5629, 0.4517)	1.1663 (0.5922, 0.4474)	1.0033 (0.0948, 0.0762)
		$S(t_0)$	0.2729 (0.1508, 0.3664)	0.3254 (0.1175, 0.2894)	0.3314 (0.0309, 0.0762)
		$h(t_0)$	12.5930 (66.8758, 3.1211)	19.8978 (330.8525, 5.5566)	3.2242 (0.3057, 0.0786)
		π_1	0.3408 (0.1417, 0.3498)	0.3347 (0.1473, 0.3613)	0.3337 (0.0368, 0.0902)
	L	θ	2.1952 (1.8995, 0.9602)	1.3081 (1.5392, 0.7996)	1.5111 (0.0695, 0.0377)
		λ_1	0.5265 (0.3889, 0.5938)	0.6608 (0.4734, 0.6943)	0.5063 (0.0677, 0.1096)
		λ_2	1.0067 (0.6038, 0.4642)	1.3056 (0.7064, 0.5250)	1.0128 (0.0929, 0.0739)
		$S(t_0)$	0.3040 (0.1342, 0.3279)	0.3259 (0.1171, 0.2849)	0.3277 (0.0314, 0.0767)
		$h(t_0)$	4.9113 (5.8069, 0.7317)	4.0849 (5.7042, 0.5719)	3.2627 (0.3361, 0.0847)
		π_1	0.3420 (0.1514, 0.3683)	0.3331 (0.1588, 0.3851)	0.3333 (0.0369, 0.0894)
	M	θ	2.3217 (2.4361, 1.0846)	1.3362 (2.0291, 0.8898)	1.5048 (0.0632, 0.0360)
		λ_1	0.5202 (0.3623, 0.5357)	0.6293 (0.4277, 0.6170)	0.5051 (0.0675, 0.1081)
		λ_2	0.9819 (0.5469, 0.4240)	1.2256 (0.6334, 0.4668)	1.0039 (0.0916, 0.0733)
		$S(t_0)$	0.2929 (0.1424, 0.3529)	0.3340 (0.1222, 0.3015)	0.3308 (0.0315, 0.0777)
		$h(t_0)$	82.1588 (2333.2308, 25.1153)	1417.5874 (44600.3335, 445.7707)	3.2312 (0.3194, 0.0832)
		π_1	0.3457 (0.1471, 0.3541)	0.3389 (0.1531, 0.3672)	0.3347 (0.0364, 0.0872)
	R	θ	3.9964 (4.4007, 2.0684)	2.1679 (3.0716, 1.2524)	1.5049 (0.0397, 0.0212)
		λ_1	0.4167 (0.3236, 0.5273)	0.5472 (0.3449, 0.5278)	0.5011 (0.0672, 0.1086)
		λ_2	0.8367 (0.5703, 0.4611)	1.1146 (0.5566, 0.4137)	1.0057 (0.0974, 0.0793)
		$S(t_0)$	0.2378 (0.1830, 0.4588)	0.3215 (0.1310, 0.3252)	0.3313 (0.0318, 0.0781)
		$h(t_0)$	6367.0680 (195746.3820, 2004.2364)	2212348.4107 (66784263.7750, 696692.2290)	3.2269 (0.3071, 0.0792)
		π_1	0.3344 (0.1427, 0.3486)	0.3303 (0.1464, 0.3563)	0.3326 (0.0366, 0.0891)
(30, 15)	U	θ	2.4631 (1.9703, 0.9909)	1.3752 (1.4962, 0.7913)	1.5081 (0.0553, 0.0299)
		λ_1	0.4598 (0.2747, 0.4356)	0.5756 (0.3070, 0.4548)	0.5010 (0.0714, 0.1121)
		λ_2	0.9333 (0.4576, 0.3693)	1.1710 (0.4951, 0.3779)	1.0073 (0.1007, 0.0797)
		$S(t_0)$	0.2897 (0.1165, 0.2800)	0.3299 (0.0912, 0.2186)	0.3302 (0.0326, 0.0788)
		$h(t_0)$	5.3565 (5.9008, 0.8253)	4.1917 (5.0317, 0.6063)	3.2319 (0.3226, 0.0819)
		π_1	0.3306 (0.1177, 0.2743)	0.3299 (0.1185, 0.2763)	0.3322 (0.0395, 0.0922)
	L	θ	1.8065 (1.3532, 0.6977)	1.0650 (1.2850, 0.7249)	1.5030 (0.0765, 0.0414)
		λ_1	0.5156 (0.3220, 0.4974)	0.6398 (0.3804, 0.5693)	0.5018 (0.0720, 0.1152)
		λ_2	1.0087 (0.4932, 0.3936)	1.2663 (0.5805, 0.4515)	1.0026 (0.0974, 0.0781)
		$S(t_0)$	0.3265 (0.1032, 0.2510)	0.3359 (0.0925, 0.2239)	0.3317 (0.0337, 0.0825)
		$h(t_0)$	3.6590 (1.8600, 0.3534)	3.1470 (1.5111, 0.3008)	3.2147 (0.3437, 0.0873)
		π_1	0.3353 (0.1294, 0.3108)	0.3343 (0.1305, 0.3131)	0.3336 (0.0402, 0.0968)
	M	θ	1.9975 (1.5884, 0.7977)	1.1277 (1.3645, 0.7559)	1.5054 (0.0699, 0.0383)
		λ_1	0.5037 (0.2903, 0.4553)	0.6042 (0.3334, 0.5123)	0.5031 (0.0761, 0.1230)
		λ_2	0.9774 (0.4516, 0.3535)	1.1816 (0.5060, 0.3810)	0.9995 (0.1006, 0.0815)
		$S(t_0)$	0.3096 (0.1130, 0.2759)	0.3425 (0.1007, 0.2501)	0.3320 (0.0346, 0.0865)
		$h(t_0)$	4.4768 (4.5215, 0.6153)	3.5719 (3.8817, 0.4915)	3.2168 (0.3469, 0.0891)
		π_1	0.3388 (0.1285, 0.3070)	0.3375 (0.1299, 0.3099)	0.3347 (0.0413, 0.0986)
	R	θ	3.0478 (3.0331, 1.4961)	1.5955 (2.0760, 0.9979)	1.5061 (0.0423, 0.0226)
		λ_1	0.4486 (0.2713, 0.4380)	0.5642 (0.2908, 0.4360)	0.5047 (0.0738, 0.1166)
		λ_2	0.8891 (0.4620, 0.3764)	1.1196 (0.4439, 0.3430)	1.0065 (0.0996, 0.0789)
		$S(t_0)$	0.2583 (0.1502, 0.3619)	0.3282 (0.1077, 0.2622)	0.3297 (0.0321, 0.0789)
		$h(t_0)$	14.2287 (78.5500, 3.6737)	31.8458 (365.5646, 9.3639)	3.2368 (0.3181, 0.0801)
		π_1	0.3363 (0.1169, 0.2687)	0.3350 (0.1186, 0.2722)	0.3339 (0.0395, 0.0909)

Table S12. Small-sample study: Average confidence/credible length and coverage probability (ACL, CP) for $(n, m) = (20, 10)$ and $(30, 15)$ under all four censoring schemes, $(T_1, T_2) = (0.4, 0.8)$, $G = 1{,}000$. Nominal level: 95%.

(n,m)	Scheme	Param	ACI-MLE	HPD Bayes I	HPD Bayes II
(20, 10)	U	θ	6.7640 (0.8248)	4.2917 (0.7030)	1.0326 (1.0000)
		λ_1	1.0694 (0.8096)	1.1975 (0.9020)	0.5250 (1.0000)
		λ_2	1.8505 (0.8136)	1.9450 (0.9230)	0.7529 (1.0000)
		$S(t_0)$	0.4181 (0.8310)	0.4205 (0.9180)	0.2377 (1.0000)
		$h(t_0)$	43.9021 (0.9684)	68.0029 (0.8890)	2.4780 (1.0000)
		π_1	0.5403 (0.8971)	0.4900 (0.8800)	0.2842 (1.0000)
	L	θ	4.7605 (0.8131)	3.1451 (0.6760)	1.0261 (1.0000)
		λ_1	1.2499 (0.8604)	1.3925 (0.9120)	0.5349 (1.0000)
		λ_2	2.1406 (0.8655)	2.2742 (0.9370)	0.7684 (1.0000)
		$S(t_0)$	0.4668 (0.8480)	0.4263 (0.9080)	0.2378 (1.0000)
		$h(t_0)$	9.1625 (0.9507)	7.0886 (0.9110)	2.4908 (0.9980)
		π_1	0.5554 (0.8737)	0.4987 (0.8510)	0.2869 (1.0000)
	M	θ	4.8448 (0.7908)	3.1004 (0.6260)	1.0274 (1.0000)
		λ_1	1.1830 (0.8622)	1.2828 (0.9050)	0.5307 (1.0000)
		λ_2	1.9805 (0.8684)	2.0322 (0.9330)	0.7596 (1.0000)
		$S(t_0)$	0.4413 (0.8255)	0.4218 (0.9110)	0.2389 (1.0000)
		$h(t_0)$	394.2711 (0.9367)	2643.0785 (0.8270)	2.4855 (1.0000)
		π_1	0.5569 (0.9031)	0.5027 (0.8850)	0.2864 (1.0000)
	R	θ	9.9813 (0.8077)	5.8224 (0.6920)	1.0483 (1.0000)
		λ_1	1.0178 (0.7794)	1.1380 (0.8930)	0.5241 (0.9990)
		λ_2	1.8189 (0.7955)	1.8746 (0.9320)	0.7528 (1.0000)
		$S(t_0)$	0.4508 (0.7733)	0.4391 (0.9060)	0.2398 (0.9970)
		$h(t_0)$	65506.7567 (0.9302)	870413.4452 (0.8450)	2.5185 (0.9970)
		π_1	0.5348 (0.8836)	0.4881 (0.8730)	0.2837 (1.0000)
(30, 15)	U	θ	5.3342 (0.8778)	3.3694 (0.7150)	1.0269 (1.0000)
		λ_1	0.9598 (0.8457)	1.0230 (0.9300)	0.4964 (0.9960)
		λ_2	1.7041 (0.8547)	1.6575 (0.9320)	0.7148 (1.0000)
		$S(t_0)$	0.3810 (0.8878)	0.3621 (0.9430)	0.2234 (0.9980)
		$h(t_0)$	11.3883 (0.9709)	8.1365 (0.8870)	2.3529 (0.9970)
		π_1	0.4549 (0.9048)	0.4256 (0.9030)	0.2679 (1.0000)
	L	θ	3.8569 (0.8596)	2.4695 (0.6420)	1.0015 (1.0000)
		λ_1	1.1012 (0.8495)	1.1726 (0.9090)	0.5048 (1.0000)
		λ_2	1.9188 (0.8877)	1.8840 (0.9210)	0.7254 (0.9990)
		$S(t_0)$	0.4037 (0.9178)	0.3685 (0.9440)	0.2233 (0.9980)
		$h(t_0)$	5.0563 (0.9488)	3.8951 (0.8800)	2.2947 (0.9970)
		π_1	0.4753 (0.8987)	0.4423 (0.8960)	0.2724 (1.0000)
	M	θ	4.0361 (0.8243)	2.5893 (0.6350)	1.0180 (1.0000)
		λ_1	1.0163 (0.8504)	1.0629 (0.9170)	0.5014 (0.9990)
		λ_2	1.6792 (0.8876)	1.6579 (0.9280)	0.7172 (1.0000)
		$S(t_0)$	0.3834 (0.8725)	0.3615 (0.9270)	0.2250 (0.9990)
		$h(t_0)$	7.8120 (0.9317)	5.6115 (0.8140)	2.3442 (0.9970)
		π_1	0.4685 (0.8916)	0.4364 (0.8870)	0.2710 (0.9990)
	R	θ	7.6025 (0.8072)	4.2935 (0.6440)	1.0438 (1.0000)
		λ_1	0.9616 (0.8353)	0.9992 (0.9150)	0.4984 (0.9990)
		λ_2	1.6993 (0.8404)	1.5856 (0.9340)	0.7133 (1.0000)
		$S(t_0)$	0.4326 (0.8564)	0.3907 (0.9270)	0.2263 (0.9990)
		$h(t_0)$	54.6652 (0.9157)	94.1600 (0.7990)	2.4072 (0.9980)
		π_1	0.4575 (0.8936)	0.4274 (0.8900)	0.2683 (1.0000)

Table S13. Alternative-parameter study: Average point estimates (RMSE, MRAB) for two true parameter configurations under the uniform (U) and right-heavy (R) schemes, $(T_1, T_2) = (0.4, 0.8)$, $G = 1{,}000$, using the profile MLE and the weakly informative Bayes I prior. Configuration $(0.5, 1.0, 0.5)$: $S_0(t_0) = 0.4265$, $h_0(t_0) = 1.9260$, and $\pi_{10} = 0.6667$. Configuration $(3.0, 0.25, 0.75)$: $S_0(t_0) = 0.3133$, $h_0(t_0) = 4.4817$, and $\pi_{10} = 0.2500$.

$(\theta_0, \lambda_{10}, \lambda_{20})$	(n, m)	Scheme	Param	MLE	Bayes I
(0.5, 1.0, 0.5)	(40, 20)	U	θ	1.1673 (1.3332, 1.9500)	0.5871 (0.8162, 1.1156)
			λ_1	0.9385 (0.3677, 0.2945)	1.0709 (0.3525, 0.2673)
			λ_2	0.4613 (0.2319, 0.3702)	0.5265 (0.2341, 0.3616)
			$S(t_0)$	0.4042 (0.1009, 0.1863)	0.4189 (0.0862, 0.1608)
			$h(t_0)$	2.6237 (1.8963, 0.4812)	2.2357 (1.5425, 0.3239)
			π_1	0.6707 (0.1095, 0.1309)	0.6707 (0.1095, 0.1308)
		R	θ	1.5394 (2.0317, 2.7316)	0.8002 (1.3304, 1.4824)
			λ_1	0.8863 (0.3707, 0.3054)	1.0096 (0.3247, 0.2537)
			λ_2	0.4491 (0.2234, 0.3625)	0.5125 (0.2194, 0.3396)
			$S(t_0)$	0.3848 (0.1241, 0.2155)	0.4159 (0.0948, 0.1695)
			$h(t_0)$	3.9205 (10.8112, 1.1576)	3.6788 (17.1207, 1.0788)
			π_1	0.6628 (0.1089, 0.1314)	0.6628 (0.1089, 0.1314)
	(80, 40)	U	θ	0.8097 (0.8132, 1.2289)	0.4121 (0.5588, 0.8476)
			λ_1	0.9515 (0.2568, 0.2034)	1.0480 (0.2357, 0.1818)
			λ_2	0.4838 (0.1618, 0.2599)	0.5335 (0.1623, 0.2550)
			$S(t_0)$	0.4212 (0.0637, 0.1173)	0.4271 (0.0582, 0.1074)
			$h(t_0)$	2.1671 (0.7450, 0.2360)	1.9579 (0.5839, 0.1763)
			π_1	0.6634 (0.0731, 0.0858)	0.6634 (0.0731, 0.0858)
		R	θ	1.1020 (1.2622, 1.8577)	0.5775 (0.8160, 1.0933)
			λ_1	0.9385 (0.2674, 0.2153)	1.0325 (0.2385, 0.1859)
			λ_2	0.4686 (0.1668, 0.2716)	0.5154 (0.1618, 0.2543)
			$S(t_0)$	0.3991 (0.0818, 0.1440)	0.4186 (0.0660, 0.1188)
			$h(t_0)$	2.5956 (1.6301, 0.4519)	2.2201 (1.2927, 0.3017)
			π_1	0.6676 (0.0766, 0.0925)	0.6676 (0.0766, 0.0924)
(3.0, 0.25, 0.75)	(40, 20)	U	θ	3.5977 (1.7268, 0.4314)	2.4633 (1.9653, 0.5476)
			λ_1	0.2476 (0.1508, 0.4535)	0.3316 (0.2118, 0.6095)
			λ_2	0.7473 (0.3435, 0.3557)	1.0097 (0.5135, 0.5362)
			$S(t_0)$	0.2813 (0.1033, 0.2597)	0.3205 (0.0883, 0.2243)
			$h(t_0)$	6.3810 (5.4287, 0.5916)	5.2863 (5.4232, 0.5769)
			π_1	0.2501 (0.0968, 0.3022)	0.2491 (0.0979, 0.3057)
		R	θ	3.9013 (2.4953, 0.6444)	2.4914 (2.4200, 0.6899)
			λ_1	0.2380 (0.1514, 0.4775)	0.3196 (0.1932, 0.5846)
			λ_2	0.7191 (0.3668, 0.3891)	0.9634 (0.4561, 0.4964)
			$S(t_0)$	0.2708 (0.1273, 0.3217)	0.3345 (0.1060, 0.2834)
			$h(t_0)$	8.4028 (12.3659, 1.1290)	7.4258 (17.4842, 1.1477)
			π_1	0.2494 (0.0960, 0.3008)	0.2494 (0.0960, 0.3012)
	(80, 40)	U	θ	3.2619 (1.1023, 0.2879)	2.6502 (1.3861, 0.3674)
			λ_1	0.2483 (0.1017, 0.3194)	0.2959 (0.1381, 0.4085)
			λ_2	0.7589 (0.2497, 0.2583)	0.9057 (0.3677, 0.3657)
			$S(t_0)$	0.2965 (0.0659, 0.1641)	0.3169 (0.0605, 0.1536)
			$h(t_0)$	5.1745 (2.0535, 0.2962)	4.6189 (2.0309, 0.3115)
			π_1	0.2479 (0.0678, 0.2155)	0.2480 (0.0677, 0.2157)
		R	θ	3.3875 (1.5943, 0.4129)	2.3444 (1.8773, 0.5282)
			λ_1	0.2435 (0.1063, 0.3322)	0.3057 (0.1398, 0.4321)
			λ_2	0.7448 (0.2631, 0.2741)	0.9367 (0.3681, 0.3938)
			$S(t_0)$	0.2912 (0.0900, 0.2216)	0.3349 (0.0859, 0.2278)
			$h(t_0)$	5.8541 (4.0330, 0.5233)	4.9182 (3.9573, 0.5416)
			π_1	0.2468 (0.0670, 0.2133)	0.2468 (0.0670, 0.2136)

Table S14. Alternative-parameter study: Average confidence/credible length and coverage probability (ACL, CP) for two true parameter configurations under the uniform (U) and right-heavy (R) schemes, $(T_1, T_2) = (0.4, 0.8)$, $G = 1{,}000$. Nominal level: 95%. True values as in Table S13.

$(\theta_0, \lambda_{10}, \lambda_{20})$	(n, m)	Scheme	Param	ACI-MLE	HPD Bayes I
(0.5, 1.0, 0.5)	(40, 20)	U	θ	2.9305 (0.6940)	1.6497 (0.6350)
			λ_1	1.3838 (0.8850)	1.2626 (0.9370)
			λ_2	0.8325 (0.8420)	0.8072 (0.9040)
			$S(t_0)$	0.3916 (0.8740)	0.3115 (0.9230)
			$h(t_0)$	3.8321 (0.9630)	2.6865 (0.9420)
			π_1	0.4009 (0.9050)	0.3807 (0.8830)
		R	θ	4.2999 (0.6710)	2.3284 (0.6250)
			λ_1	1.3964 (0.8660)	1.2026 (0.9260)
			λ_2	0.8324 (0.8520)	0.7808 (0.9030)
			$S(t_0)$	0.3981 (0.9130)	0.3284 (0.9260)
			$h(t_0)$	9.2818 (0.9600)	8.2634 (0.9310)
			π_1	0.4001 (0.9210)	0.3808 (0.9000)
	(80, 40)	U	θ	2.0232 (0.7450)	1.1470 (0.6410)
			λ_1	0.9996 (0.9140)	0.9001 (0.9520)
			λ_2	0.6252 (0.9060)	0.5951 (0.9430)
			$S(t_0)$	0.2756 (0.9070)	0.2225 (0.9420)
			$h(t_0)$	2.0337 (0.9560)	1.5274 (0.9190)
			π_1	0.2906 (0.9360)	0.2829 (0.9340)
		R	θ	3.0663 (0.6940)	1.6536 (0.6070)
			λ_1	1.0572 (0.8990)	0.8965 (0.9410)
			λ_2	0.6385 (0.8910)	0.5813 (0.9280)
			$S(t_0)$	0.3034 (0.9360)	0.2383 (0.9380)
			$h(t_0)$	4.1965 (0.9520)	2.5492 (0.9180)
			π_1	0.2875 (0.9210)	0.2801 (0.9210)
(3.0, 0.25, 0.75)	(40, 20)	U	θ	5.7341 (0.9458)	4.5583 (0.7490)
			λ_1	0.5222 (0.8604)	0.6197 (0.9020)
			λ_2	1.2930 (0.8775)	1.4019 (0.8680)
			$S(t_0)$	0.3277 (0.8936)	0.3267 (0.9390)
			$h(t_0)$	11.7728 (0.9669)	9.3756 (0.7960)
			π_1	0.3618 (0.8855)	0.3402 (0.8780)
		R	θ	7.4840 (0.9060)	5.2268 (0.6990)
			λ_1	0.5168 (0.8070)	0.5922 (0.9040)
			λ_2	1.3337 (0.8340)	1.3120 (0.8600)
			$S(t_0)$	0.3961 (0.8850)	0.3694 (0.9070)
			$h(t_0)$	21.2778 (0.9360)	19.5301 (0.7350)
			π_1	0.3618 (0.8930)	0.3413 (0.8920)
	(80, 40)	U	θ	4.0598 (0.9430)	3.8059 (0.8250)
			λ_1	0.3951 (0.9100)	0.4357 (0.9170)
			λ_2	0.9294 (0.9160)	1.0164 (0.8610)
			$S(t_0)$	0.2403 (0.9340)	0.2399 (0.9490)
			$h(t_0)$	6.3684 (0.9680)	5.6287 (0.8650)
			π_1	0.2629 (0.9430)	0.2543 (0.9330)
		R	θ	5.5822 (0.9480)	4.3930 (0.7570)
			λ_1	0.4137 (0.8900)	0.4493 (0.9160)
			λ_2	1.0130 (0.9090)	1.0342 (0.8250)
			$S(t_0)$	0.3144 (0.9140)	0.2925 (0.8850)
			$h(t_0)$	11.2266 (0.9520)	8.7780 (0.7750)
			π_1	0.2627 (0.9490)	0.2539 (0.9360)

To examine whether the qualitative findings depend on the particular data-generating values, the simulation was repeated under two further true parameter configurations chosen to sit well away from the baseline $(\theta_0, \lambda_{10}, \lambda_{20}) = (1.5, 0.5, 1.0)$: A near-exponential design $(0.5, 1.0, 0.5)$ with a slowly increasing hazard and $\pi_{10} = 2/3$, and a strongly accelerating design $(3.0, 0.25, 0.75)$ with $\pi_{10} = 1/4$. Both were run under the uniform (U) and right-heavy (R) schemes for $(n, m) = (40, 20)$ and $(80, 40)$, with $(T_1, T_2) = (0.4, 0.8)$ and $G = 1{,}000$ replications, using the objective profile MLE and the weakly informative Bayes I procedure (The moderately informative Bayes II prior is centered at the baseline truth and is therefore not carried over to these alternative configurations). Tables S13 and S14 report the point and interval estimation results. The structural conclusions of Section 6 carry over unchanged: θ and $h(t_0)$ remain the hardest quantities to estimate, and their point estimators and delta-method intervals deteriorate sharply under the right-heavy scheme, whereas $S(t_0)$ and π_1 are recovered accurately with close to nominal coverage under every configuration. The relative risk π_1, in particular, is estimated essentially without bias in both designs, consistent with its direct identifiability from the observed cause counts.